sustainability

MDPI

Article

Alkali–Silica Reactivity Potential of Aggregates from Different Sources in Pakistan

Muhammad Yousaf [1], Muhammad Shajih Zafar [2,*], Muhammad Usman [1], Muhammad Usama [1], Muhammad Usman Yousaf [1], Gianluca Scaccianoce [3], Laura Cirrincione [3] and Marco Vocciante [2,*]

[1] Department of Civil Engineering, University of Engineering and Technology, Lahore 54890, Pakistan; yousaf_dr786@uet.edu.pk (M.Y.); 2019msces34@student.uet.edu.pk (M.U.); 2019civ86@student.uet.edu.pk (M.U.); 2024msces131@student.uet.edu.pk (M.U.Y.)
[2] Department of Chemistry and Industrial Chemistry, University of Genova, Via Dodecaneso 31, 16146 Genova, Italy
[3] Department of Engineering, University of Palermo, Viale delle Scienze Bld. 9, 90128 Palermo, Italy; gianluca.scaccianoce@unipa.it (G.S.); laura.cirrincione@unipa.it (L.C.)
* Correspondence: shajih.zafar@gmail.com (M.S.Z.); marco.vocciante@unige.it (M.V.)

Abstract: This paper aims to support stakeholders in the sustainable construction sector by exploring the potential of unexamined aggregates from five distinct origins: the Jandol River, the Swat River, the Panjkorha River, the Kitkot Drain, and the Shavey Drain situated in Malakand division, North Waziristan, Pakistan, concerning Alkali–Silica Reaction (ASR) prior to their incorporation into large-scale construction practices. Petrographic examination for the determination of the mineralogical composition of all collected aggregates revealed that aggregates stemming from the Swat River, Panjkorh River, Kitkot Drain, and Shavey Drain exhibited no reactive minerals. In contrast, those from the Jandol River showed reactive mineral content. Physical analysis of the aggregates revealed that Jandol River aggregates had superior resistance to impact, crushing, and abrasion, having values of 18.53%, 18.53%, and 20.10%, respectively. Moreover, the chemical analysis exhibited the highest silica content (SiO_2) in Jandol River aggregates, i.e., 94.7%, respectively. Samples in the form of cubes, prisms, and mortar bars were prepared to study both the mechanical properties and the expansion tendencies of specimens prepared from different aggregate sources. Validation of the reactive nature of the Jandol River aggregates was corroborated by the expansion results obtained from the mortar bars and the reduction in compressive strength and flexure strength by 8.2% and 9.2%, respectively, after 90 days, higher than that of aggregates exposed to ASR sourced from the other four origins. It can be asserted that aggregates from the Jandol River source are more susceptible to ASR as compared to other aggregates. To mitigate the potential of ASR, various strategies, such as using low reactivity, natural, or processed aggregates; low alkali-containing cement; inducing pozzolanic substances in concrete; etc., are recommended. Simultaneously, an economic feasibility study and environmental assessments are recommended as future developments.

Keywords: circular economy; alkali–silica reactivity; petrographic analysis; sustainable concrete

Academic Editor: Laura Moretti

Received: 17 February 2025
Revised: 23 March 2025
Accepted: 28 March 2025
Published: 3 April 2025

Citation: Yousaf, M.; Zafar, M.S.; Usman, M.; Usama, M.; Yousaf, M.U.; Scaccianoce, G.; Cirrincione, L.; Vocciante, M. Alkali–Silica Reactivity Potential of Aggregates from Different Sources in Pakistan. *Sustainability* **2025**, *17*, 3203. https://doi.org/10.3390/su17073203

1. Introduction

Nowadays, global concern about human activities is increasing more and more. Various sectors of modern civilization, such as process industries, transportation networks, and agricultural applications, intensely disturb the surroundings, frequently instigating the uninterrupted or unintended discharge of carbon-based and inorganic contaminants [1].

Such operations, frequently characterized by inappropriate waste-dumping procedures and no sufficient source retrieval [2,3], result in imparting progressively and noteworthy negative influence upon bionetworks and humanoid wellbeing [4,5]. The necessity to comprehend such complications has led to the advancement of an extensive variety of physicochemical and biotic methodologies for the retrieval of polluted waters [6–10] and soils [11–14].

Favorably, a quick progress of knowledge has also enhanced the emphasis on green technologies to handle anthropic development and depletion of natural assets in a sustainable manner [15–17]. Such practices bring building engineering into the field of sustainable constructions. As of today, the construction industry relies majorly on concrete as its foremost constituent, the ingredients of which include cement, which is the most widely used, fine aggregates (sand), coarse aggregates (gravel/crushes), and water. The enormous use of concrete for building is because of many properties, including strength, practicality and cost-effectiveness, given by the fact that it can be poured on site, has low maintenance costs, and the ease of finding the ingredients for its production. However, the growing demand for cement is accelerating the demand for its raw materials, particularly limestone, which is essential for the production of Portland cement, the type of cement used in concrete for more than 200 years. Such depletion of unrenewable assets is a serious distress as life and ecological concerns rise [18], since the greenhouse gas emissions produced result in global over-heating [19]. In order to take care of such problems, scientists and experts are searching for substances which can partly or completely substitute cementitious materials in the concrete mixture without compromising its behavior and robustness [20,21] while also taking into account sustainability-related aspects, such as the use of local raw materials to ease the economic and environmental burdens of production processes [22]. At the same time, extending as far as possible the longevity and structural integrity of buildings currently constructed of concrete is also becoming increasingly critical.

The phenomenon known in the concrete field as Alkali–Silica Reaction (ASR) involves a chemical process in which hydroxyl ions, prevalent within the pore fluid of concrete, react with the silica present in certain aggregates [23,24]. This interaction results in the formation of an Alkali–Silica gel. Remarkably, the gel itself maintains a commendable degree of stability and does not inherently bring breakages or additional impacts. However, when exposed to aqueous environments, this gel undergoes swelling [25]. Consequently, this expansion and swelling of the gel initiates stress within the concrete matrix, ultimately leading to the formation of interior micro ruptures or breakages [26]. The trio of chemical reactions described by Equations (1)–(3) outlines the intricate three-step progression of ASR working [23]. Firstly, the powerful hydroxyl ions (OH^-) exert their influence by cleaving the robust siloxane bonds (Si-O-Si), thereby mobilizing the conversion of feeble silicic acid to alkali silicate or Alkali–Silica gel, as shown in Equations (1) and (2). Subsequently, the ingress of water prompts the consequent alkali–silicate gel expansion, a phenomenon articulated in Equation (3).

$$\underset{}{\text{Si-O-Si} + R^+ + OH^-} \rightarrow \underset{\text{Alkali silicate}}{\text{Si-O-R}} + \underset{\text{Silicic acid}}{\text{H-O-Si}} \quad (1)$$

$$\underset{\text{Silicic acid}}{R^+ + OH^- + \text{H-O-Si}} \rightarrow \underset{\text{Alkali silicate}}{\text{Si-O-R}} + H_2O \quad (2)$$

$$\text{Si-O-R} + nH_2O \rightarrow \text{Si-O}^-\text{-}(H_2O)_n + R^+ \quad (3)$$

Manifestly, the sustained occurrence of the reaction depends on the concurrent interaction of three pivotal components: the presence of reactive particles within the aggregate, encompassing opal, quartzite, and chert; a sufficient amount of alkalis within the cement;

and a wellspring of moisture. The absence of any one component of this triad is sufficient to inhibit the progression of the reaction. Over the past several decades, a great deal of research has been conducted on the Alkali–Silica reaction (ASR). Stanton stands as a pioneering figure, being among the first to recognize and investigate the intricacies of the ASR within concrete [27]. In terms of its tangible manifestations on concrete, the ASR produces a spectrum of effects, including ruptures, enlargements, and alterations in mechanical characteristics. These effects, resultingly, hasten the worsening of the useability, robustness, and load-bearing capacity of concrete structures [28]. These occurrences, of course, result in a shorter useful life of the material, thus leading not only to a not-negligible expenditure of economic and energy resources necessary for the restoration of the building structures in which they are used but also to as many significant pollutant emissions resulting from the necessary renovation and/or (in the worst case scenario) dismantling, disposal, and replacement of the damaged materials [29,30]. To mitigate the effects of ASR, four prominent strategies have been studied:

i. Utilizing less reactive aggregates.
ii. Using cement containing a lower concentration of alkali.
iii. Using pozzolanic substances such as slag [31], fly ashes [32], silica fume [33], etc.
iv. Incorporation of lithium carbonates [34] and lithium nitrates.

Among the aforementioned strategies to alleviate the potential of ASR, the use of less reactive aggregates is the most desirable approach [35]. Where there exists a tedious task to locate the less reactive aggregates taking into account the expenditure and accessibility, the second option can be opted for as the second most desirable method.

There exists a profound bond between ASR, ASR-induced damages, and sustainable development. As discussed earlier, concrete is the widely used material because of its capacity to withstand heavy loads and robustness that endures for years. ASR is basically a fatal illness of the concrete that reduces its durability and life span. For instance, if a concrete structure is erected to withstand all kinds of loads for a period of 100 years, the influence of ASR may reduce it to 50 years, or if the intensity exceeds, the structure may require rehabilitation even after 5–10 years. This is where the consumption of raw materials would become a point of serious concern. The maintenance cost would not only be an economic consideration, but the environmental impacts of repairs due to cracking and expansion also pose a threat to sustainable development. The use of additional energy, material transportation, manufacturing, and consumption of raw materials for the purpose of the rehabilitation of structures would defy the norms of sustainable development because the production of cement is linked to the emission of carbon dioxide in the atmosphere, which is responsible for global warming. Construction and demolition waste due to damage repair would cause significant waste management issues. Therefore, ASR is a mechanism that not only causes deterioration of the concrete structure before time, causing safety concerns for the building inhabitants, but also is a source responsible for the rapid depletion of the natural resources, posing a threat for the future generations.

The evolution and proliferation of microcracks is generally considered to be the underlying catalyst for alterations in material properties [36]. Given the pivotal role of concrete mechanical properties in the assessment of structural integrity, serviceability, and capacity, the influence of ASR on these properties has been thoroughly investigated via experimental, numerical, and analytical inquiries. For example, Munir et al. [37] have documented a significant reduction in compressive strength, with Mach Hills aggregates experiencing a pronounced decline of 22% under ASTM C1260 [38] exposure conditions, while Tuguwali aggregates showed a slightly lesser reduction of 16% under comparable conditions. In addition, Munir et al. [37] elucidated the discernible impact of the aggregate source on the overall flexural strength loss, which ranged from 22% to 34% for samples subjected to

the ASTM C1260 [38] test. In a parallel investigation, Marzouk et al. [39] found a notable 24% reduction in compressive strength over 84 days for normal-strength concrete samples vulnerable to a NaOH solution. Moreover, they observed a corresponding reduction in flexural strength of up to 24% related to mildly sensitive aggregates, while Ghafoori et al. [40] elucidated a decline in the concrete cylinders compressive strength attributed to ASR in samples containing reactive aggregates. The results of these investigations unveiled that the compressive strength initially exhibited limited sensitivity to ASR in the early stages; however, significant degradation was observed in the later stages, coinciding with extreme expansions and crack formation. Okpin et al. [41], using a variety of testing standards, explored the corruption of mechanical properties in concrete casts with three distinct aggregate typologies. Their results highlighted the variability in compressive strength over the duration of the tests, with concrete strength showing a gradual increase up to 28 days, followed by a subsequent decline.

Mortar bar expansion is a common method used to evaluate concrete degradation due to ASR. A multitude of standard methods are used worldwide to measure ASR expansion, providing insights into the aggregates reactivity. In particular, the expedite mortar bars test stands as the most widely utilized method worldwide. Originally introduced in 1986 by Oberholster and Davis [42], this test has since gained widespread acceptance as an accelerated means of assessing aggregate ASR. In such a test, mortar bars are immersed in a strong alkaline solution (1 N NaOH) for at least 14 days at 80 °C, as required by ASTM C1260 [38]. Conversely, ASTM C227 [43] represents an alternative method with a long-established history in ASR detection, requiring nearly six months to complete [32]. Moreover, the exposure constraints outlined in ASTM C227 [43] are not rigorous enough to induce ASR in less time. As a result, the current investigation used ASTM C1260 [38] to evaluate the ASR potential of locally sourced aggregates that have not been previously studied. A multitude of previous investigations have examined the physical and engineering properties of local aggregates, as evidenced by the synthesis presented in Table 1. However, there is a lack of literature regarding the ASR potential of local aggregates complying with ASTM C1260 [38,44].

Table 1. Preceding literature on locally available aggregates.

Year	Studied Aggregates/Rock Formation	Test Performed	Results and Findings	Ref.
2022	Shalozan, Abbott abad, Orakzai agency, Swabi, and Sada	Physical and chemical properties, cube prism and accelerated mortar bar expansion, compressive strength, flexural strength, crushing strength, Los Angles abrasion, and impact test, petrographic analysis.	Physical properties of aggregates were within the specified ranges of ATSM standards. Swabi aggregates showed the highest resistance to crushing, abrasion, and impact. Orakzai and Shalozan aggregates have higher silica content, making them more reactive for ASR. Orakzai aggregates expanded by 0.119% at 14 days and 0.201% at 28 days, indicating reactivity. Specimens with Orakzai aggregates had a 9% decrease in flexural strength under ASR exposure compared to other sources.	[44]
2020	Sakesar limestone, Pail Padhrar, Tobar valley, Dhak pass.	Los Angeles abrasion value, soundness test, aggregate impact, aggregate crushing, specific gravity, and unit weight.	Aggregates from the Dhak Pass and Pail Padhar exhibited remarkably low abrasion values. The aggregates from Tobar Valley and Pail Padhar proved to be suitable options for the pavement surface course. In addition, the water absorption, specific gravity, and unit weight characteristics of all aggregates were within acceptable standards.	[45]
2018	Chakdara quarry, Katkala quarry, Gulabad Khwar, Pajkor River at Rani.	Specific gravity, water absorption, bulk density, flakiness index, elongation index, soundness, crushing value, impact value, Los Angeles abrasion, and concrete cylinder strength.	The quartet of extracted materials exhibited a diverse range of characteristics, consisting of specific gravity, bulk density, and water absorption, which ranged from 2.67 to 2.72, 99 lb/ft^3 to 101 lb/ft^3, and 1.58% to 1.92%, respectively. Flakiness and elongation indices ranged from 21.1% to 25.1% and 14.7% to 24.2%, respectively. Soundness tests gave results between 3.35% and 5.04%. Aggregates from the Gulabad quarry emerged as star performers in both the crushing and impact tests, recording the most commendable values of 13.23% and 16.56%, respectively. Among the tested sources, the Gulabad aggregate had the highest concrete cylinder strength (2376 psi).	[46]

Table 1. *Cont.*

Year	Studied Aggregates/Rock Formation	Test Performed	Results and Findings	Ref.
2018	The area around Loni Kot (Karachi-Hyderabad Motorway).	Particle size, water absorption, bulk density, solidity, organic impurities, clay lumps, friable particles, flakiness and elongation index, Los Angeles abrasion test, crushing value, and impact value.	Approximately 77% of the fine particles were reported to be free of organic impurities. Coarse aggregates exhibited water absorption rates ranging from 0.20% to 0.60%, while their fine counterparts exhibited a wider range of 0.40% to 2.20%. Specific gravity for fine aggregates ranged from 2.42 to 2.72 and for coarse aggregates from 1.95 to 2.87. Notably, 25% and 27% of the coarse aggregates were identified as flaky and elongated particles, respectively. The impact value and aggregate crushing value were 25% and 28%, respectively.	[47]
2017	The Kamser Mountains from Muzaffarabad in Kashmir, the Jhelum River at the Lehri Mangla, the Sheikh Hills, Tuguwali Hills, and Mach Hills from the Sargodha region.	Expansion test, petrographic analysis.	According to ASTM C227, aggregates sourced from the Sargodha region exhibited mortar bar expansion values ranging from 0.05% to 0.07%. In stark contrast, aggregates sourced from the Jhelum and Kamser regions exhibited significantly lower expansion rates, falling below 0.04%. However, a concerning revelation emerged during the ASTM C1260 test, where all aggregates from the Sargodha region showed reactivity, with expansions exceeding the critical threshold of 0.20%. This unsettling trend was confirmed by petrographic analysis, further highlighting the risk posed by these aggregates.	[48]
2017	Sargodha, Mangla, and Margalla crush, as well as Banalla crush.	Specific gravity, water absorption, bulk density, impact value, concrete cylinder strength, splitting tensile strength, and flexural.	Margalla crushes exhibited the most remarkable specific gravity among the samples, while Sargodha and Barnala crushes exhibited lower water absorption rates compared to Margalla and Mangla crushes. Interestingly, Margalla crush exhibited the lowest bulk density within the group. Sargodha Crush exhibited the lowest impact value (11.6%) and crushing value (17.9%) among all the samples. Conversely, Margalla crushes demonstrated the maximum flexural capacity (4.90 MPa) and compressive capacity (26.3 MPa) among the tested aggregates. Barnala crushed stone exhibited the highest splitting tensile strength within the evaluated parameters.	[49]
2016	Malikhore formation (Lasbela and Khuzdar districts).	Compressive strength, Los Angeles abrasion, flakiness, elongation index, bulk density, Alkali–Silica reactivity, and petrographic analysis.	The results showed a specific gravity of 2.74 and a water absorption rate of only 0.28%. Impressively, the compressive strength increased to 6179 psi, while the Los Angeles abrasion test showed a value of 23%. Given these robust properties, the aggregates were considered well suited for concrete production, as confirmed by petrographic analysis.	[50]
2015	Obhan Shah quarry (OSQ), Chattan Shah quarry (CSQ), Goal Pahari quarry (GPQ), Darak quarry (DQ) and Jara Takar quarry (JTQ).	Specific gravity, bulk density, flakiness and elongation index, water absorption, crushing value, impact value, abrasion value, and compressive strength	Each of the aggregate sources had specific gravities that met the established standards, but their bulk densities remained below 2400 kg/m^3. All sources exceeded the specified limit of 15% for the flakiness index. The water absorption, crush, impact, and abrasion values of each source were within acceptable parameters. Notably, JTQ had the lowest compressive strength of 20.8 MPa, while CSQ had the most remarkable 28-day compressive strength, rising to an impressive 38.2 MPa.	[51]
2014	Limestones from Margala Hill (MH), Lockhart (LT), Kawagarh (KW), Sammana Suk (SM), and Shekhai (SH).	Los Angeles abrasion, impact value, flakiness index, elongation index, density, water absorption, and petrographic analysis	All mechanical and physical properties were well within the tolerances of both BS and ASTM standards. Among them, KW had the highest specific gravity. Kawagarh and Sammana Suk exhibited the lowest Los Angeles abrasion values and impact values, respectively.	[52]
2013	Hajra, Kamser, Arja, Margalla and Sargodha crush.	Unit weight, flakiness and elongation index, impact value, crushing value, compressive strength, tensile strength specific gravity, water absorption.	The three Kashmiri sources, namely Hajra, Kamser, and Arja, exhibited specific gravities that fell within the spectrum delineated by the Margalla and Sargodha crushes. Kamser and Hajra had the lowest water absorption rates among the Kashmiri sources. All Kashmiri sources exhibited flakiness and elongation indices towel within the BS standards. The impact values ranged from 10 to 15%, while the crushing values ranged from 15 to 23%. The Kamser aggregates had the lowest compressive and tensile strength values, while the Arja aggregates had the highest values for both compressive and tensile strength.	[53]
2012	Bara River, Basi, LoyeKhawar, Zangali/JaniKhawar	Los Angeles abrasion, ASR, Petrographic examination, Bulk density, Soundness.	Aggregate samples from the Bara River, Basi, Zangali, and Loye Khawar showed a spectrum of bulk densities ranging from 2.3 to 3.1. The soundness test revealed a tapestry of values that resonated with the intrinsic character of each quarry: 13.05, 6.61, 8.94, and 17.69. Abrasion test revealed their resilience with values of 21.2, 18.5, 24, and 20, respectively, crafting a narrative of endurance and strength. No expansion was observed, each sample standing as a testament to its harmlessness. Delicate strokes of petrographic analysis then painted a portrait of purity, revealing reactive carbonates or the shadow of unstable silica.	[54]

Table 1. *Cont.*

Year	Studied Aggregates/Rock Formation	Test Performed	Results and Findings	Ref.
2009	Jurana formation, Sakesar limestone	Specific gravity, water absorption, soundness test, Los Angeles abrasion, moisture content.	The specific gravities ranged from 2.62 to 2.70, with water absorption ranging from a minimum of 0.44% to a slightly higher 1.30%. After five immersion cycles, the soundness test revealed a spectrum from 2.15% to 8.47%, indicating of the aggregates. Abrasion values, ranging from 18.6% to 29.4%, underscored their durability. Maximum dry density went from 143 to 144.8 pounds per cubic foot, while optimum moisture content was found to be 5.4% to 5.6%. These results underscore the suitability of the tested aggregates for road construction.	[55]
2009	Allai aggregate	Bulk density, specific gravity, water absorption and ASR.	Although the techical properties of the aggregates were within standard limits, their potential for Alkali–Silica reaction was noted. As a precautionary measure, it is recommended that these aggregates be incorporated into concrete mixes along with mitigating agents such as fly ash, slag, and low alkali cement. This strategic approach aims to minimize the risk of Alkali–Silica reactions and ensure the durability and longevity of concrete structures.	[56]
2008	Girdue limestone, Sakhi Sarwar, Pitok quarry, Uzman quarry at Nullah Zungi, Khalgeri Mullah quarry	Specific gravity, water absorption, soundness test, Los Angeles abrasion, moisture content, CBR value.	Specific gravities ranged from 2.61 to 2.69 and water absorption from 0.57% to 1.65%. Soundness test values ranged from 1.80 to 3.77%, while abrasion values ranged from 17.9% to 30.6%. Maximum dry density ranged from 143.7 to 144.9 lb/ft^3, with optimal damp concentration observed between 5.2% and 5.4%. Notably, the California bearing ratio ranged from 84.4% to 99.2%, indicating favorable conditions for surface preparation and concrete work, particularly sourced from the Girdu formation.	[57]
2006	Chiniot, Margala, Sikhanwali, Takial and Khairabad.	Crushing value, abrasion value, specific gravity, porosity and particle shape index.	Crush values ranged from 21.78% to 29.20%, while the Los Angeles abrasion values were from 16.3% to 25.46%. Impact values ranged from 12.73% to 18.65%. Upon close inspection, the Margala and Chiniott sources emerged as paragons of minimalism, boasting the lowest porosity, crushing value, and impact value, compared to the grandeur of the highest specific gravity values. However, amidst this tapestry of attributes, the Margalla source aggregate emerged with regal distinction, adorned with the highest quotient of flaky and elongated particles, adding complexity to its narrative.	[58]

Based on the above, with the aim to investigate and expand the range of possible local, hence more sustainable, sources that are adequate for construction lacking degradation of mechanical properties and with minimal environmental impact, the current study was designed to investigate the performance of locally available aggregates with respect to ASR. Specifically, aggregate samples were sourced from five pits located in the northwestern region (Malakand Division) of Pakistan, chosen for their anticipated utilization in large-scale building practices like dams. Anyway, it should be recognized that the mechanical properties of concrete erections are profoundly affected by ASR. Hence, initial testing of unexplored aggregates concerning ASR is the most effective technique to prevent concrete deterioration in mega construction. In the preliminary phase, a petrographic examination of the assessed aggregates was performed to elucidate their mineral composition and reactive constituents. Subsequently, cube, prism, and mortar bar samples were prepared and were made vulnerable to ASR solutions, according to ASTM C1260 [38]. Parallel samples were also cast and cured using standard water conditions for comparison purposes. The focal point of this research lies in determining the extent of concrete deterioration induced by the incorporation of unexplored aggregates, as measured by ASR expansion and subsequential loss of mechanical property under ASTM C1260 compliant exposure conditions. This investigation stands as a pioneering effort, not only in assessing the ASR susceptibility of unexplored aggregates but also in providing stakeholders with the necessary confidence and technical insight to employ local aggregates in large-scale projects. Furthermore, the research seeks to expand the repertoire of viable local aggregate sources for construction practices, ensuring compatibility without compromising mechanical properties. From

the literature reported earlier, it is evident that a greater number of studies have been conducted for the determination of technical properties of the local aggregates; however, limited literature is presented for the probability of ASR in local aggregates, particularly under ASTM C1260. Moreover, no investigation has been conducted before to determine the ASR potential of the aggregates sourced from Malakand Division in Pakistan, i.e., Swat River, Panjkorha River, Jandol River, Kitkot Drain, and Shavey Drain.

The novelty of the study under consideration is that it has investigated the potential of ASR in the aforementioned locally available aggregates which were yet to be explored before. Moreover, this study has commenced the investigation under ASTM C1260, on which limited literature is available, rendering it distinct. From the perspective of sustainable development of the construction industry, this work is part of an initial investigation in order to determine whether such materials are structurally reliable, before proceeding with the subsequent environmental (e.g., comparison with other materials used for the same purpose in terms of carbon footprint and pollutant emissions) and economic (e.g., quantity of material available and potential scale of production) analyses.

2. Materials and Methods

2.1. Materials and Specimen Preparation

The investigation under consideration examined five various aggregate sources for Alkali–Silica reactivity. These aggregates sourced from the Swat River, Panjkorha River, Jandool River, Shavey Drain, and Kitkot Drain, are an integral part of the contemporary landscape of large-scale projects in the local construction sector, as outlined in Tables 2 and 3. The selected aggregates, namely those sourced from the Swat River, Panjkorha River, Jandool River, Shavey Drain, and Kitkot Drain, were obtained through controlled blasting operations conducted over various geological formations within their respective vicinities. After the blasting phase, a dry crushing process was used to break up large rock formations into smaller, more manageable aggregates. Once the true representative aggregates were collected from their designated locations, further grading procedures were enacted according to ASTM C1260 [38]. Ordinary Portland cement served as the binding agent in these experiments, while a blend was made utilizing tap water. Portland Cement was kindly provided by Maple Leaf cement, Pakistan. Lithium carbonates and Lithium nitrates were purchased from city scientific Pakistan.

Table 2. Site of locally available aggregates.

Sr. No.	Aggregate Sources	Latitude	Longitude
1	Swat River (Naseeb crush plant chakdara)	34°41′24″ N	72°01′47″ E
2	Panjkorha (river Malik and ko block crush shakwali temargara)	34°47′28″ N	71°48′48″ E
3	Kitkot khwar (Mamund block factory Barkaly)	34°47′31″ N	71°24′16″ E
4	Shavey khwar (Bilal crush plant Dir)	34°51′48″ N	71°40′4.9″ E
5	Jandool river (raghagan dam water resort salarzai)	34°46′23″ N	71°37′06″ E

Table 3. Aggregate samples.

Aggregate Sources	Crusher Site	Aggregate Sample
River Swat aggregates		
River Panjkorha aggregate		
River Jandool aggregates		
Shavey Drain aggregates		
Kitkot Drain aggregates		

2.2. Experimental Procedures

Various assessments were undertaken to ascertain the engineering characteristics of the cement utilized in this study. These tests included the soundness test, performed according to EN 196-3 [59], to evaluate the resistance of the cement to volume change upon hydration. The Blaine air permeability test, according to ASTM C204 [60], was used to determine the specific surface area of the cement particles, which provides insight into their fineness. In addition, the fineness test, assessed by the percentage of cement particles passing through a #200 sieve, was performed according to ASTM C184 [61]. The setting time, a critical parameter affecting construction schedules, was determined according to ASTM C191 [62]. Finally, the standard consistency of the cement, which indicates the quantity of water essential to attain the desired consistency, was measured according to ASTM C187 [63]. A series of tests were conducted on the aggregates employed in this study to measure both their physical and chemical characteristics. Such assessments contained the BS-812-112 [64] impact value test, which is designed to gauge the material's resistance to sudden force application. The BS-812-110 [65] test for crushing value was utilized to ascertain the ability of the aggregates to withstand crushing loads. Furthermore, the ASTM C535 [66] abrasion test was utilized to evaluate the abrasion resistance of the aggregates. The determination of bulk density and void ratio was executed in accordance with ASTM C29 [67], providing crucial insights into the compactness and void spaces within the aggregate matrix. Specific water absorption and gravity characteristics were evaluated according to ASTM C127 [68], providing insight into the density of the material and its propensity to absorb moisture. Chemical analysis of the aggregates was carried out on powdered samples according to the guidelines of ASTM C114 [69]. It was worth determining the chemical composition of the local aggregates at the initial stage, as it can predict the intensity of ASR in the concrete and its subsequent impacts. The extent of reactive silica attained through chemical analysis existing in the aggregates leads to a rigorous reaction with alkalis present in the cement, and its consequent exposure to moisture can result in intensive cracking and degradation of the concrete structure in due course, an outcome of ASR. Therefore, chemical analysis of local aggregates can be considered an essential prediction of the possible ASR in the concrete. In addition, petrographic analysis was performed according to the ASTM C295 [70] standard. For the petrographic analysis, the samples first underwent a thorough washing process to eliminate extraneous contaminants, followed by an examination aimed at identifying different rock typologies through petrographic modal analysis, performed using both low and high magnification settings. Fine sections were then meticulously made and investigated under a polarizing microscope to identify any deleterious constituents within the aggregate matrix. The petrographic microscope employed for this purpose was an Olympus BX41TF equipped with a DP12 digital camera to ensure accurate documentation and analysis. Expansion measurements were meticulously recorded on mortar bar specimens at specified intervals of 3, 7, 14, 28, 56, and 90 days. Prior to each measurement, the digital length comparator readings were carefully calibrated using a standardized bar. Compressive strength tests on cubes were performed according to ASTM C109 [71] using a prescribed a 1000 N/s loading rate. Similarly, flexural strength tests on prisms were performed according to ASTM C348 [72] with a 2640 N/s loading rate. Test ages corresponded to intervals of 3, 7, 14, 28, 56, and 90 days after ASR exposure at 80 °C. For comparative analysis, parallel indistinguishable samples were prepared and cured in water and then tested under analogous conditions. Figure 1 outlines the sequential steps of the specimen preparation and testing procedures.

Figure 1. Preparation and evaluation of specimens: (**a**) electric mixer; (**b**) molds on vibrating table; (**c**) cast samples; (**d**) samples in ASR solution; (**e**) samples inside oven and tested with digital length comparator.

After demolding, the mortar bar expansion specimens were subjected to initial length measurements using a length comparator according to the procedures outlined in ASTM C490 [73]. These specimens were then immersed in water at 80 °C for 24 h, after which the length changes were again measured with the length comparator. The mortar bar samples were then transferred to a NaOH solution maintained at 80 °C. At specified intervals corresponding to the target ages, the extent of length change was meticulously determined. The change in length was calculated employing Equation (4) and then expressed as a percentage:

$$L = \frac{Lx - Li}{G} \quad (4)$$

where Li, L, Lx, and G are the initial value, expansion at the target age, length comparator value at the desired age, and gauge length, respectively.

Field Emission Scanning Electron Microscope (FESEM) inspection was used to investigate the microcracking and related damage observed in the tested samples. The FESEM instrument used was a Sigma 500VP manufactured by Carl Zeiss (Jena, Germany). Fragments between 3 and 5 mm in size, obtained from samples containing different aggregates, were meticulously selected for FESEM examination. Before being placed in the specimen holder of the FESEM, these fragments underwent gold coating using a sputter-coating equipment to improve conductivity and imaging quality. Subsequently, the specimen fragments were analyzed at various magnifications to obtain comprehensive visual data. Figure 2 demonstrates the process flow of the study under consideration.

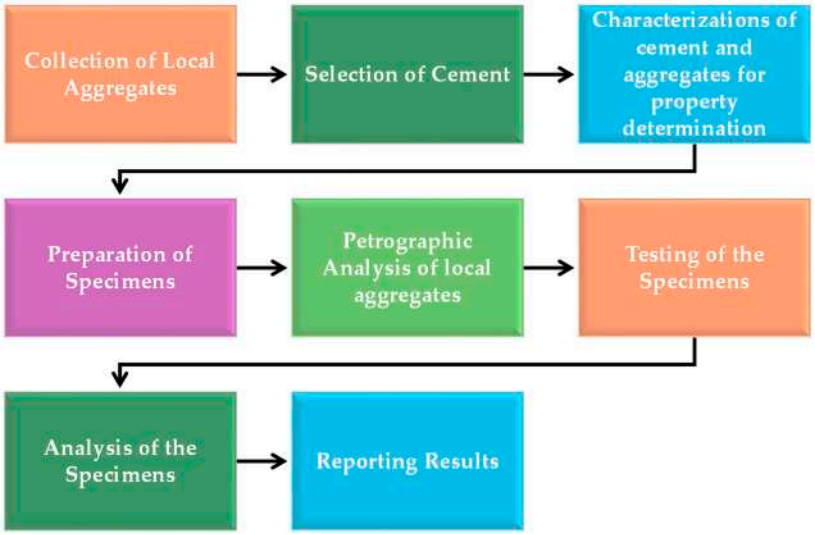

Figure 2. Process flow of the study under consideration.

3. Results and Discussion

3.1. Cement and Coarse Aggregates Characteristics

The outcomes of the tests on physical properties of the cement are presented in Table 4. It is noteworthy that all such physical properties were found to be within the permissible ranges established by both ASTM and European (EN) standards, according to the research findings. For example, the initial setting time was more than 45 min, and the final setting time was less than 375 min, whereas the surface area and fineness of the cement were more than 2250 cm^2/g and 90%, respectively, in accordance with the criteria established by the ASTM standards.

Table 4. Cement physical characteristics.

Characteristic	Reference Standard	Value	Reference Limit
Standard Consistency	ASTM C187 [63]	26%	---
Initial Setting Time	ASTM C191 [62]	85 min	>45 min
Final Setting Time	ASTM C191 [62]	175 min	<375 min
Fineness (Passing #200)	ASTM C184 [61]	98.6%	≥90%
Fineness (Blaine Air Permeability)	ASTM C204 [60]	2996 cm^2/g	≥2250 cm^2/g
Soundness	EN 196-3 [59]	0.80 mm	≤10 mm

Table 5 shows the physical properties characterizing the diverse aggregate sources. Among the aggregates studied, the results revealed a noticeable divergence in properties. Notably, for all aggregate sources, the bulk density fell within the specified reference range. Amongst these sources, the Jandool River aggregates had the highest bulk den-

sity of 1510.7 kg/m^3, while the Shavey drain source showed the lowest bulk density of 1410 kg/m^3. When comparing the Jandool River aggregate to all other aggregate sources examined, it becomes apparent that the Jandool River Aggregate exhibits a significantly higher specific gravity value of 2.79. In contrast, the Shavey drain source presents the lowest specific gravity value among the samples, standing at 2.64. Furthermore, compared to the Shavey drain aggregates, which demonstrated the highest water absorption rate amid all the specimens tested, the Swat River aggregates showcased the lowest water absorption rate, measured at just 0.59%. Guided by the BS-812-112 [64] standards, aggregates are evaluated for their robustness based on impact values, with those below 10% considered strong and stable, and those above 35% considered weak and fragile and unsuitable for construction. Similarly, adherence to the BS-812-110 [65] criterion stipulates that aggregates with crushing values below 30% are deemed suitable for construction applications. Throughout this investigation, Jandol aggregates exhibited remarkable resilience, with the greatest resistance to impact, abrasion, and crushing. Conversely, Shavey drain aggregates showed a notable susceptibility to abrasion, indicating a vulnerability in this regard. In addition, it is noteworthy that Kitkot drain aggregates exhibited only marginal values for resistance to crushing and impact, suggesting a comparatively lower level of durability in these key parameters.

Table 5. Physical characteristics of tested aggregates.

Aggregate Source	Bulk Density (kg/m^3)	Specific Gravity (---)	Water Absorption (%)	Impact Value (%)	Crushing Value (%)	Abrasion Value (%)
Swat River	1490.6	2.75	0.59	20.56	20.44	21.34
Panjkorha River	1460.4	2.72	0.61	21.56	21.56	23.12
Jandol River	1510.7	2.79	0.71	18.53	18.53	20.10
Shavey Drain	1410.0	2.64	0.97	21.54	21.54	29.87
Kitkot Drain	1430.3	2.69	0.81	27.31	27.31	28.41

Table 6 reports the outcomes of the chemical analysis performed on the aggregates. It is noteworthy that all the chemical compounds detected are within the limits prescribed by ASTM C114 [69], which underlines the compliance with the established standards. The Jandool and Swat river aggregates exhibit high silica values compared to the other sources tested, approximately 94.7% and 92.5%, respectively, while the Kitkot drain source presents a lower silica level of about 85.2%. It could be argued that the heightened silica content across all aggregate sources could lead to increased ASR expansion. Nonetheless, it is imperative to recognize that the type, size, quantity, and reactivity of silica within aggregates play a pivotal role in influencing ASR expansion and its subsequent detrimental effects [74]. Crystalline silica comprises oxygen ions and silicon tetrahedra arranged to maintain electrical neutrality, thereby yielding a more stable structure. Conversely, the porous and inherently unstable nature of amorphous silica makes it susceptible to ASR [75,76]. Furthermore, it is worth considering the potential presence of minute concentrations of reactive silica within the aggregates, rendering chemical analysis ineffective in determining their impact. In addition, the mineralogical configuration of aggregates alone may not accurately obtain the degree of impairment caused by reactive aggregates. Hence, it is strongly suggested that experimental laboratory studies be conducted under relevant standards to fully understand the performance of aggregates with respect to ASR.

Elevated Loss on Ignition values are evident in all of the examined aggregates. For example, the Loss on Ignition for the Kitkot drain aggregates was approximately 2.69%.

In accordance with ASTM C114 [69], all other aggregate constituents remained within the specified range.

Table 6. Chemical configuration of utilized aggregates.

Constituents	Swat River	Panjkora River	Jandool River	Shavey Drain	Kitkot Drain
CaO (%)	0.88	0.75	0.93	1.45	1.85
MgO (%)	0.32	0.39	0.28	0.20	0.72
SiO_2 (%)	92.5	89.9	94.7	88.4	85.2
SO_3 (%)	0.16	0.12	0.23	0.13	0.22
Al_2O_3 (%)	1.45	2.89	0.52	1.20	1.67
Fe_2O_3 (%)	0.67	0.75	0.25	0.34	0.40
L.O.I (%)	1.24	1.88	1.44	1.87	2.69

3.2. Petrographic Examination of Aggregate Sample

3.2.1. Panjkorha River Aggregates

The aggregates under investigation are classified as fine-grained limestone due to their predominant petrographic composition of finely dispersed calcite grains. Over 95% of the samples consist of calcite ($CaCO_3$) by volume. Notably, these grains have undergone partial recrystallization to microspar/spar through neomorphism. Traces of dolomite, quartz/chert, and iron ore are also detected within acceptable limits. Petrographic analysis conclusively classifies the aggregate sample as fine-grained limestone, given that the model composition exceeds 90% calcite ($CaCO_3$). Petrographic analysis of the aggregates under investigation, i.e., Panjkorha River aggregates, revealed a modal structure composition which consisted of 96% calcite, 3% chert/quartz, and 1% iron ore, as shown in Figure 3.

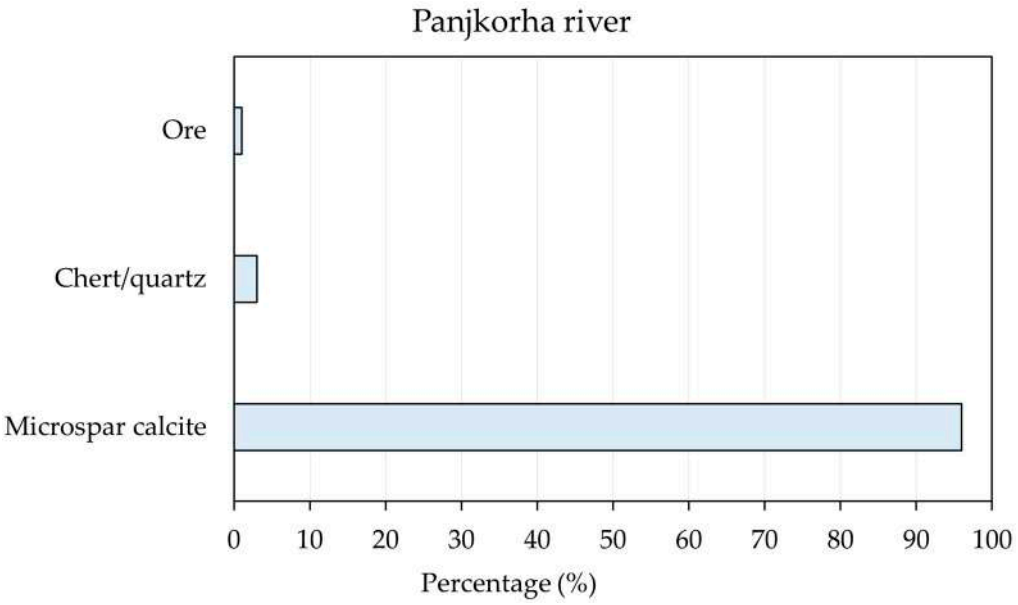

Figure 3. Panjkorha aggregates' mineralogical composition.

The supplied sample predominantly comprises 96% microspar calcite, a composition known for its resilience against the Alkali–Silica reaction (ASR), making it suitable for incorporation into asphalt and concrete mixes. However, a series of additional engineering tests—including, but not limited to, Los Angeles, water absorption, flakiness, elongation, and coating and stripping evaluations—must be rigorously conducted per project specifications to provide definitive validation of the aggregate's suitability for use.

3.2.2. Shavey Drain Aggregates

This aggregate source possesses a fine to medium grain size, going from 0.1 to 0.4 mm, and has a brownish-gray complexion when examined in hand specimens. Under petrographic scrutiny, these fragments are delineated as limestone with finely dispersed grains. Alternatively, using the Dunham classification, they could be identified as mudstone due to the sample's predominant composition of small calcite ($CaCO_3$) grains, which make up over 95% of its volume (Figure 4). Of particular note is the presence of sparry/microsparry calcite ($CaCO_3$), a phenomenon induced by the neomorphism process within the fine matrix. Furthermore, a minute fraction (about 3%) of the sample is composed of subhedral to anhedral quartz/chert grains. In the midst of this complex composition, dark-colored ores, presumably iron ores, are evident, as well as within the material.

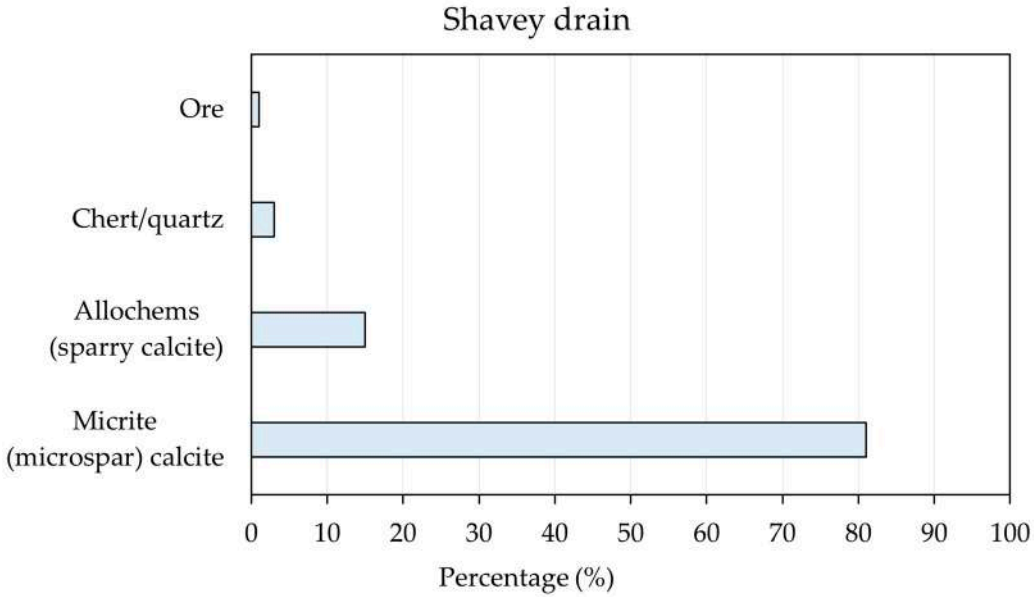

Figure 4. Shavey Drain aggregates' mineralogical composition.

The petrographic analysis indicates that the aggregate specimens analyzed are suitable for use in concrete applications. Specifically, the aggregate samples analyzed exhibit an absence of Alkali–Silica reactive (ASR) constituents, rendering them impervious to the Alkali–Silica reaction. However, in order to fully determinate their suitability as an aggregate material, a full range of standard aggregate tests—including but not limited to compressive strength, Los Angeles abrasion test, soundness, crushing value, and impact valve test—should be performed on the provided aggregate samples.

3.2.3. Kitkot Drain Aggregates

The aggregate specimen, characterized by fine to medium grains and a color spectrum ranging from dark gray to black, has been identified through petrographic analysis as Wackstone (limestone). A dominant constituent, calcite, makes up over 90% of the volume of the rock as shown in Figure 5. Notable constituents include fossil fragments (allochems), carbonate mud, and various minute particles. Bioclasts/fossil fragments range in size between 0.2 and 1.8 mm, with the lime mud portion containing finer-grained bioclasts. Some of the crushed fossil fragments have undergone partial recrystallization into microspar. Although their presence is minimal and within the acceptable limits outlined by ASTM C-295 [70], traces of quartz and chert (cryptocrystalline silica) and ore have been observed as well. In addition, microscopic calcite veins cross the rock samples, occasionally

punctuated by spots of coarse-grained, euhedral crystalline calcite. Vigorous effervescence upon exposure to dilute hydrochloric acid further attests to the plentiful of calcite ($CaCO_3$).

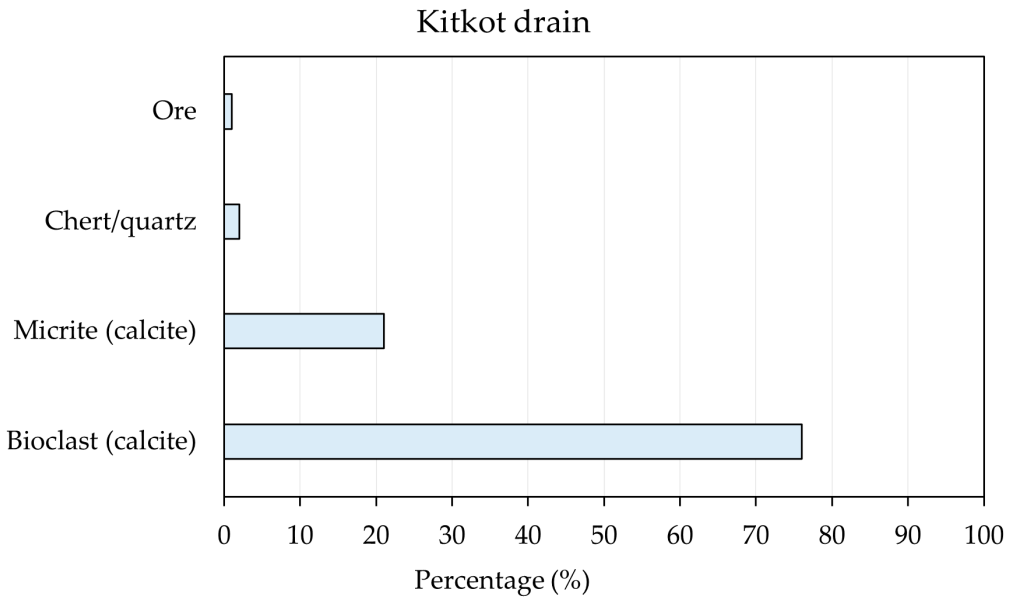

Figure 5. Kitkot Drain aggregates' mineralogical composition.

In accordance with Dunham's classification system [77], the petrographic examination of the rock sample under study categorizes it as a bioclastic limestone, specifically identified as Wackstone. With calcite ($CaCO_3$) constituting more than 90% of the limestone samples, it is considered suitable for use in concrete production and asphalt applications, provided that other essential geomechanical properties, such as loss on abrasion, water absorption, and compressive strength, meet project specifications. Due to the heterogeneous nature of the rock typologies within the quarry, the material engineer has been recommended to perform periodic evaluation of the supplied aggregates. This careful oversight ensures consistency and quality in the material supply chain.

3.2.4. Jandol River Aggregates

The aggregate under investigation is composed predominantly of quartz and feldspar, with minimal presence of clays, mafic phases (such as amphibole and pyroxene), muscovite mica, and ores. The quartz grains exhibit a wide variety of morphologies, ranging from sub-angular to sub-rounded and even subspherical. Impressively, a quarter (25%) of these quartz grains present themselves as discrete entities, forming the predominant phase of the aggregate (47%), and exhibit a deformed or a strained polycrystalline nature. Feldspar accounts for about 23% of the aggregate and is mainly present as discrete grains, many of which have undergone transformation into clays. In addition, the main opaque phases observed are magnetite/hematite, appearing as minor constituents in about 5% of the aggregate, as delineated in Figure 6.

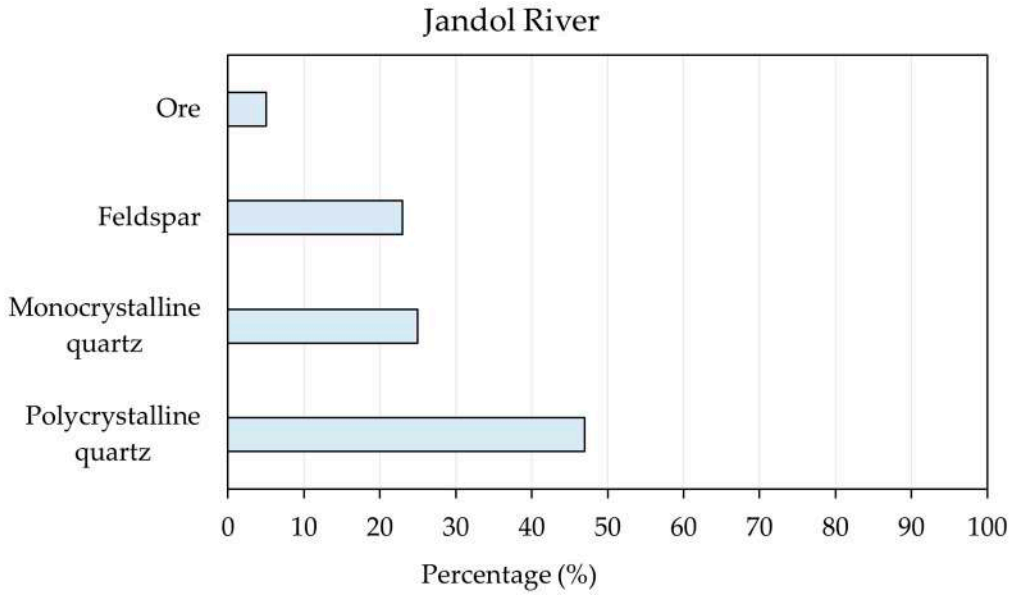

Figure 6. Jandol River aggregates' mineralogical composition.

The examined aggregate, characterized by strained quartz (deformed) and polycrystalline quartz exceeding permissible limits, presents a potential risk of Alkali–Silica reactivity (ASR). In addition, the presence of silt-sized grains in most of the aggregate samples falls within the deleterious category, further exacerbating ASR concerns. Furthermore, the presence of altered feldspar introduces a potential weakening factor to the rock strength. Petrographically, this aggregate source is not suggested for use in concrete work with ordinary Portland cement (OPC) due to its ASR potential. However, it may find application in asphalt production, provided other tests to ensure aggregate suitability, such as coating and stripping evaluations, prove successful. Prior to incorporation into any engineering work, geotechnical studies and tests—including, but not limited to, soundness, water absorption, flakiness, elongation, specific gravity, and Los Angeles abrasion test (LA)—should be conducted on the aggregate under consideration in accordance with project specifications. This rigorous analysis ensures a detailed evaluation and suitability of the aggregate for any engineering project.

3.2.5. Swat River Aggregates

The sample analyzed consists of fine-grained rock fragments that are uniform in nature and range in size from less than 0.1 to 0.3 mm. These fragments present a subdued grayish hue when observed with the naked eye. Through meticulous petrographic analysis, the sample is identified as fine-grained limestone, characterized by its microspar calcite content in excess of 90%. In addition, the presence of chert and ores within the sample is noted, contributing to its mineralogical composition. Petrographic analysis of Swat river aggregates revealed a modal structure composition dominated by 94% calcite, with 3% chert/quartz, and 3% iron ore, as shown in Figure 7.

The sample examined is primarily 94% microspar calcite, a composition known for its resistance to Alkali–Silica reaction (ASR), making it suitable for incorporation into asphalt and concrete mixes. However, a full range of other engineering tests—including, but not limited to, Los Angeles, water absorption, flakiness, elongation, and coating and stripping evaluations—must be conducted in accordance with the project specifications for these particular examined aggregates in order to provide definitive validation of the aggregate's usability.

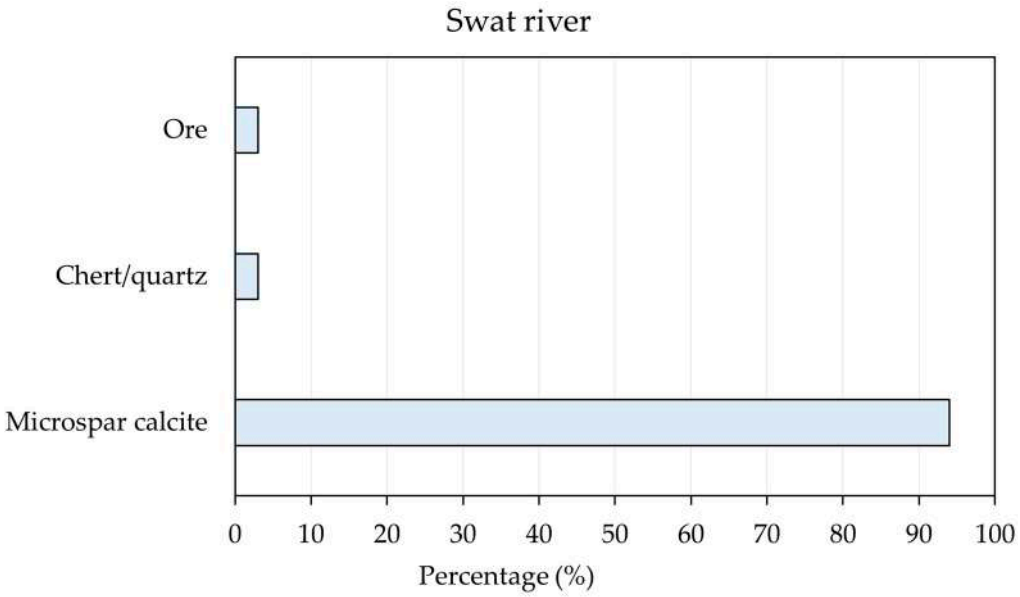

Figure 7. Swat River aggregates' mineralogical composition.

The ability of aggregates to absorb solar radiation (ASR) is influenced by several factors, including their structural type, silica content, and exposure conditions. Constituents such as opal (0.50%), cristobalite (1%), chert (3%), strained quartz (5%), and volcanic glass (3%) have been identified as susceptible to ASR [78]. Conversely, aggregates composed of dolomite and limestone, which lack reactive elements, do not promote ASR [79].

3.3. Expansion Results of Accelerated Mortar Bar

Figure 8 illustrates the expansion values derived from mortar bars. Each data point represents the mean value of five identical samples and shows a variation coefficient of less under 1.6%, well inside the limits of ASTM C1260 [38].

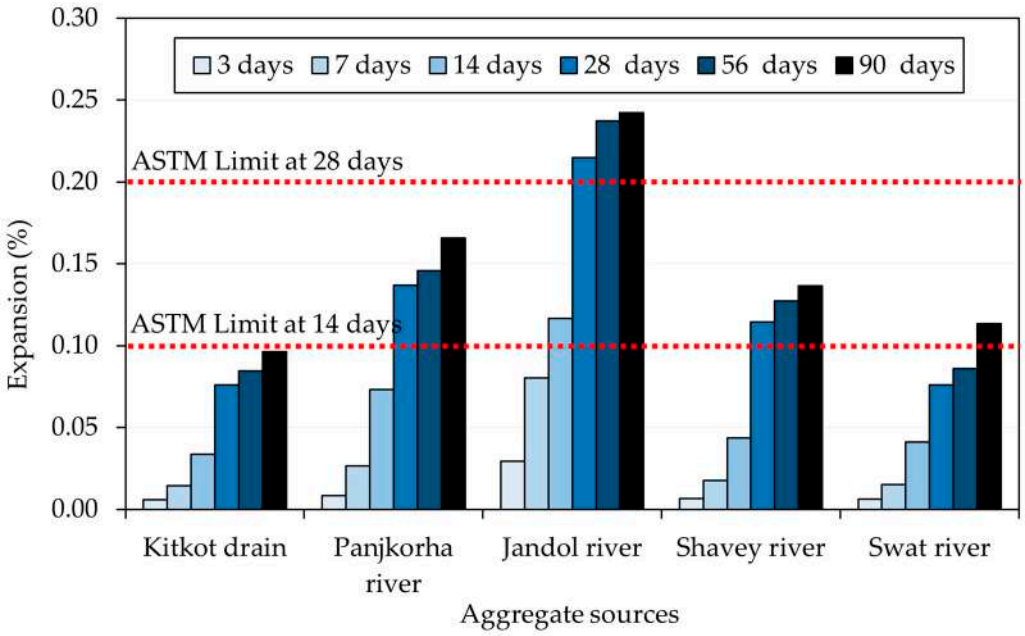

Figure 8. Expansion results of various tested aggregates.

The procured aggregate specimens were subject to a rigorous 90-day test period in accordance with ASTM C1260 standard procedures to facilitate a comprehensive examination of the results. Figure 8 shows the expansion values obtained from the accelerated

mortar bars, providing insight into the progression of the investigation. As the test period progressed, the mortar bars exhibited varying degrees of expansion, depending on the presence of reactive minerals within each aggregate source. Specifically, the Jandol source exhibited the highest expansion, reaching nearly 0.242% at the 90-day mark, due to the confirmed presence of reactive minerals, as confirmed by chemical analysis and petrographic examination of the aggregates. Conversely, the Kitkot drain source exhibited the lowest expansion, registering only 0.096% at 90 days, suggesting its non-reactive character. Similarly, the remaining aggregate sources—Panjkorha River, Shavey Drain, and Swat River aggregate sources—exhibited expansions of 0.166%, 0.137%, and 0.113%, respectively, after a 90-day exposure time under ASR circumstances (Figure 8).

It was possible to observe that the samples produced with Jandol aggregates exhibited an expansion of 0.116% at the beginning of the 14-day mark, which escalated to 0.215% by the 28th day. Meanwhile, counterparts using Kitkot, Panjkorha, Shavey, and Swat sources showed expansions of 0.034%, 0.073%, 0.044%, and 0.041%, respectively, at the initial 14-day interval. Subsequently, at the end of the 28-day period, these samples showed expansions of 0.076%, 0.137%, 0.115%, and 0.076%, respectively (Figure 9). With the exception of the Jandol River aggregates, which differed significantly, the aggregate sources, namely Swat River, Panjkorha River, Shavey Drain, and Kitkot Drain, showed expansions of less than 0.1% after the initial 14-day period, which increased to less than 0.2% by the 28th day. These expansions remained well inside the acceptable range given by ASTM C1260 [38]. Notably, the results of the petrographic examination were consistent across the board, demonstrating its critical role in predicting outcomes—a sentiment often recommended by researchers. As required by ASTM C1260 [38], the evaluation of the aggregate sources depended on their expansion rates, with thresholds set at 0.1% after 14 days and 0.2% after 28 days to represent Alkali–Silica reactivity. As a result, the tests revealed the presence of reactivity in one aggregate source (Jandol), thus identifying it as unsuitable for application under the ASTM C1260 standards. Conversely, sources such as the Swat River, Panjkorha River, Shavey Drain, and Kitkot Drain demonstrated commendable resistance to Alkali–Silica reaction, confirming their reliability. Previous research has shown that ASTM C1260 is more effective with slow-reacting aggregates.

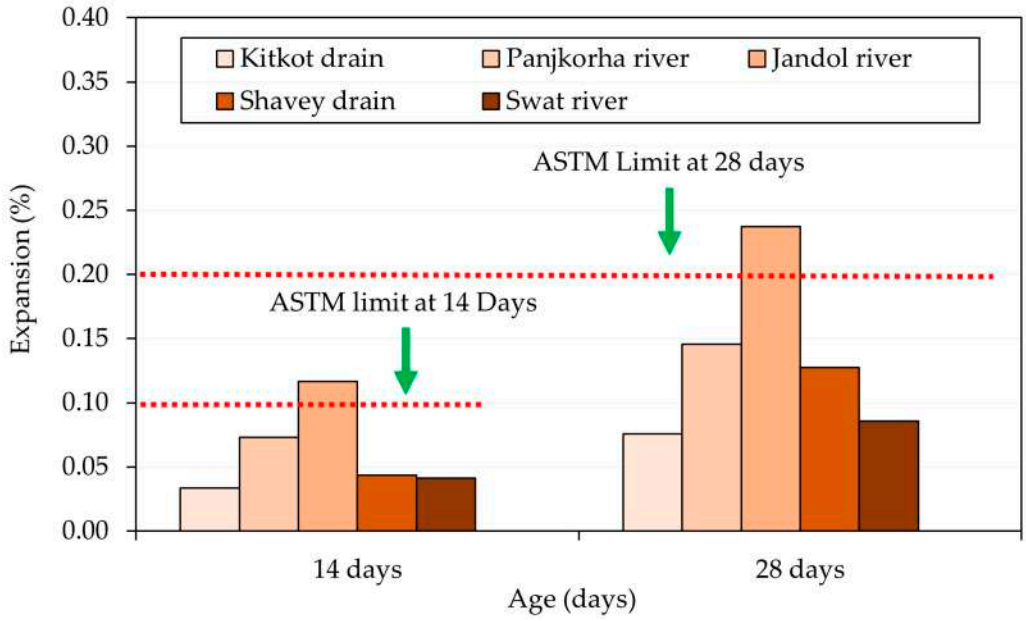

Figure 9. ASTM C1260 limits for the tested aggregates.

The narrative conveyed by Figures 10–12, captured through the lens of the SEM, offers a profound exploration of the intricate interplay between aggregate specimens and their environment, specifically in the context of the Alkali–Silica Reaction (ASR). Within this visual description, the eye is drawn to the Jandol aggregates shown in Figure 10, where microscopic cracks engrave delicate patterns across their surface. These cracks and microcracks, created by the persistent and continuous attack of ASR, reveal the silent struggle of materials subjected to environmental forces beyond their control. Figures 11 and 12 cast their gaze on specimens from the remaining aggregate sources, Kitkot, Panjkorha, Shavey, and Swat. Here, the landscape remains unspoiled and unaffected by the scars of microcracking, a testament to the inherent strength and steadfast resilience of these materials in the face of adversity.

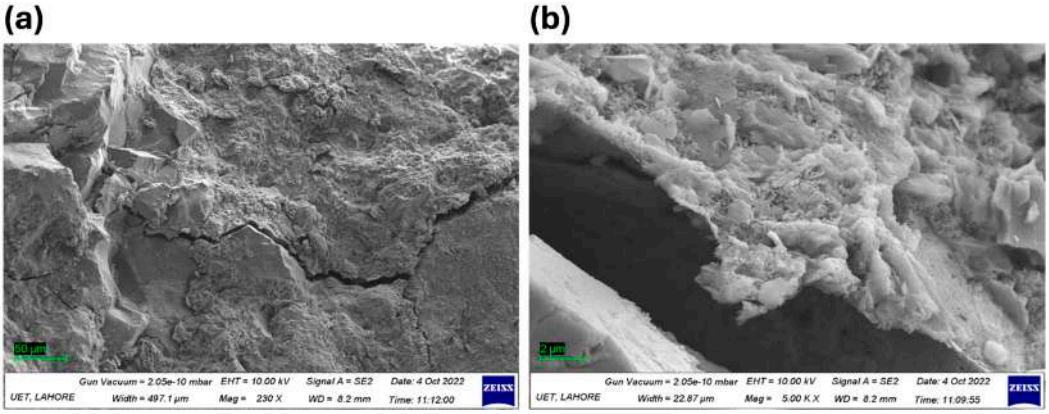

Figure 10. SEM images of specimens incorporating Jandol source aggregates at different magnifications: (**a**) 50 µm (Mag. = 230×); (**b**) 2 µm (Mag. = 5k×).

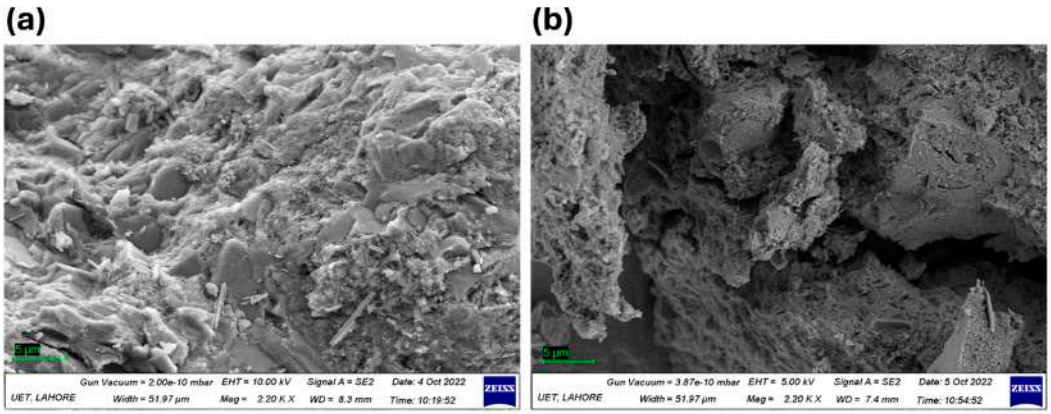

Figure 11. SEM images of specimens incorporating: (**a**) Kitkot source aggregates; (**b**) Panjkorha source aggregate.

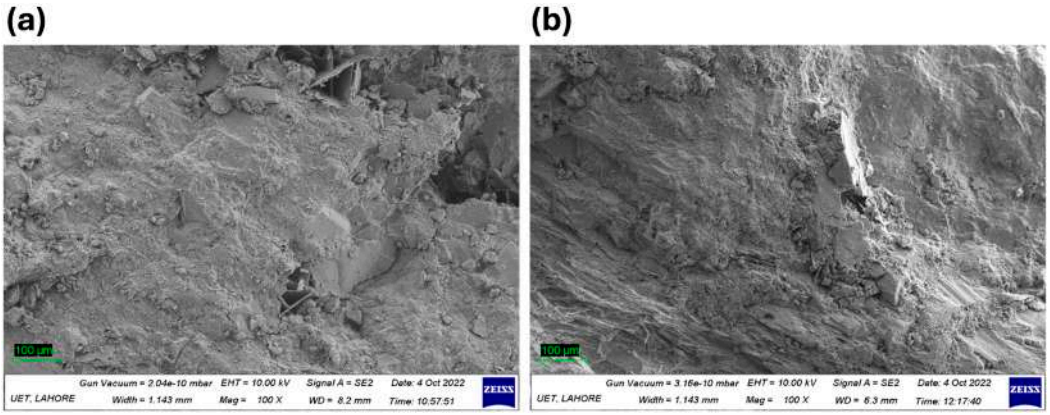

Figure 12. SEM images of specimens incorporating: (**a**) Shavey source aggregates; (**b**) Swat source aggregate.

3.4. ASR Effect on Compressive Strength

Figure 13 displays the compressive strength variation between control samples and those exposed to ASR. Overall compressive strength data were derived from the mean value of five samples to ensure robustness, with a coefficient of variation (COV) of under 1.86%. Notably, the control samples sourced from Jandool River, subjected to water curing, showed a peak compressive strength of 40.79 MPa, while the corresponding value for Shavey Drain dropped to a minimum of 25.95 MPa at the 28-day mark. At the 90-day milestone, the Shavey Drain source showed a marginal improvement, registering a minimum compressive strength of 27.20 MPa, but still lagging behind the commendable 41.23 MPa achieved by the Jandool River source.

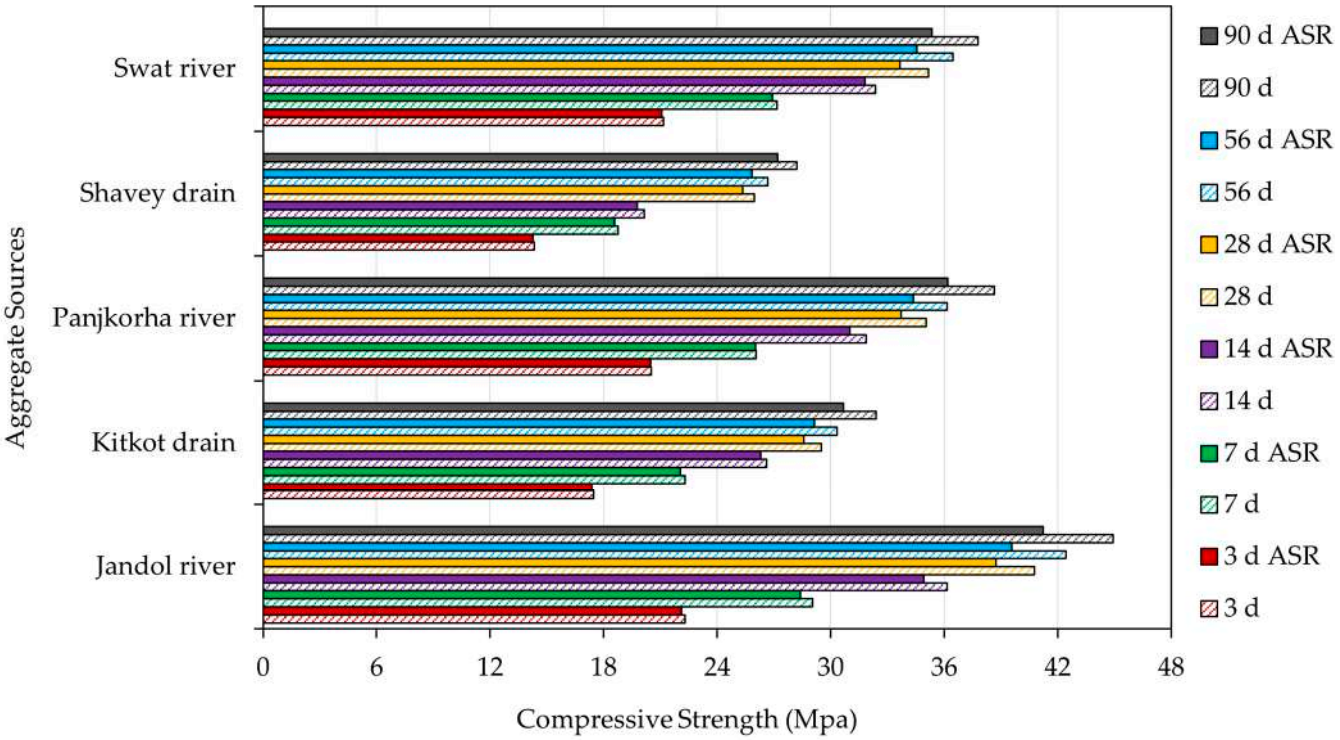

Figure 13. Effect of ASR conditions on compressive strength.

Figure 13 illustrates the difference in compressive strength between control specimens and those exposed to ASR conditions. In particular, it is evident that ASR conditions caused a reduction in compressive strength across the board. Notably, cubes made from Jandol River aggregates, which are characterized by highly reactive particles based on petrographic

examination, suffered the most significant reduction, dropping 8.2% at the 90-day point. Conversely, samples from the Shavey Drain exhibited a more modest decline, with only a 3.61% reduction in compressive strength at the same interval, due to their comparatively less reactive particle composition. Following the parameters defined by ASTM C 1260, it was found that the alternative aggregate sources, Swat River, Panjkorha River, and Kitkot Drain, exhibited a noticeable decrease in compressive strength. Specifically, reductions of 6.4%, 6.32%, and 5.31%, respectively, were documented at the 90-day mark (Figure 13). Such declines in strength could likely be attributed to the constrained expansion of the accelerated mortar bars noted earlier. However, for the Jandol River source, the strength reduction was manifested with increased severity, a phenomenon possibly caused by the onset of the ASR. Figure 14 shows the reduction in compressive strength of specimens exposed to ASR with respect to the control specimens. At an early stage of strength development, particularly at 3, 7, and 14 days, the diversity in compressive strength between control and ASR-exposed specimens is almost negligible, and subsequently the reduction in %. This may be attributed to the minimal or no effect of ASR on the concrete at its early stage of development because ASR is a slow chemical process. At early stages, the reaction is still in its initial phase, and the degree of gel formation and subsequently the expansion is negligible, and in the meantime, the concrete continues to gain strength due to hydration of cement, which occurs more rapidly. The effect of ASR becomes prominent at the later stages of concrete development when the concrete matures and ASR gains momentum. Compared to the other aggregates, the maximum strength reduction at early ages was observed for specimens containing aggregates from the Jandol River source, possibly due to the presence of more reactive minerals responsible for ASR; however, the overall impact at early stages was still less compared to the later stages of strength development.

It is also important to note that the strength loss exhibited an escalating trend over time, coinciding with the prolonged exposure to ASR conditions. Specifically, the loss of strength relative to the control mix for the Panjkorha River aggregate source jumped from 2.66% at the 14-day interval to 4.87% by the 56th day, delineating a noticeable weakening of structural integrity with prolonged exposure. Comparable reductions in compressive strength have been documented in earlier research. For instance, Munir et al. [37] elucidated a 22% loss in compressive strength for Mach Hills aggregates under ASR exposure, while the Tuguwali aggregate experienced a 16% reduction under analogous conditions. Similarly, Marzouk et al. [39] found a comprehensive 24% decrease in compressive (normal) strength for concrete after 84 days of exposure to NaOH solution. The current study confirms the diminishing effect of the ASR on compressive strength and affirms that the more reactive the aggregate source, the greater the detrimental effect on compressive strength.

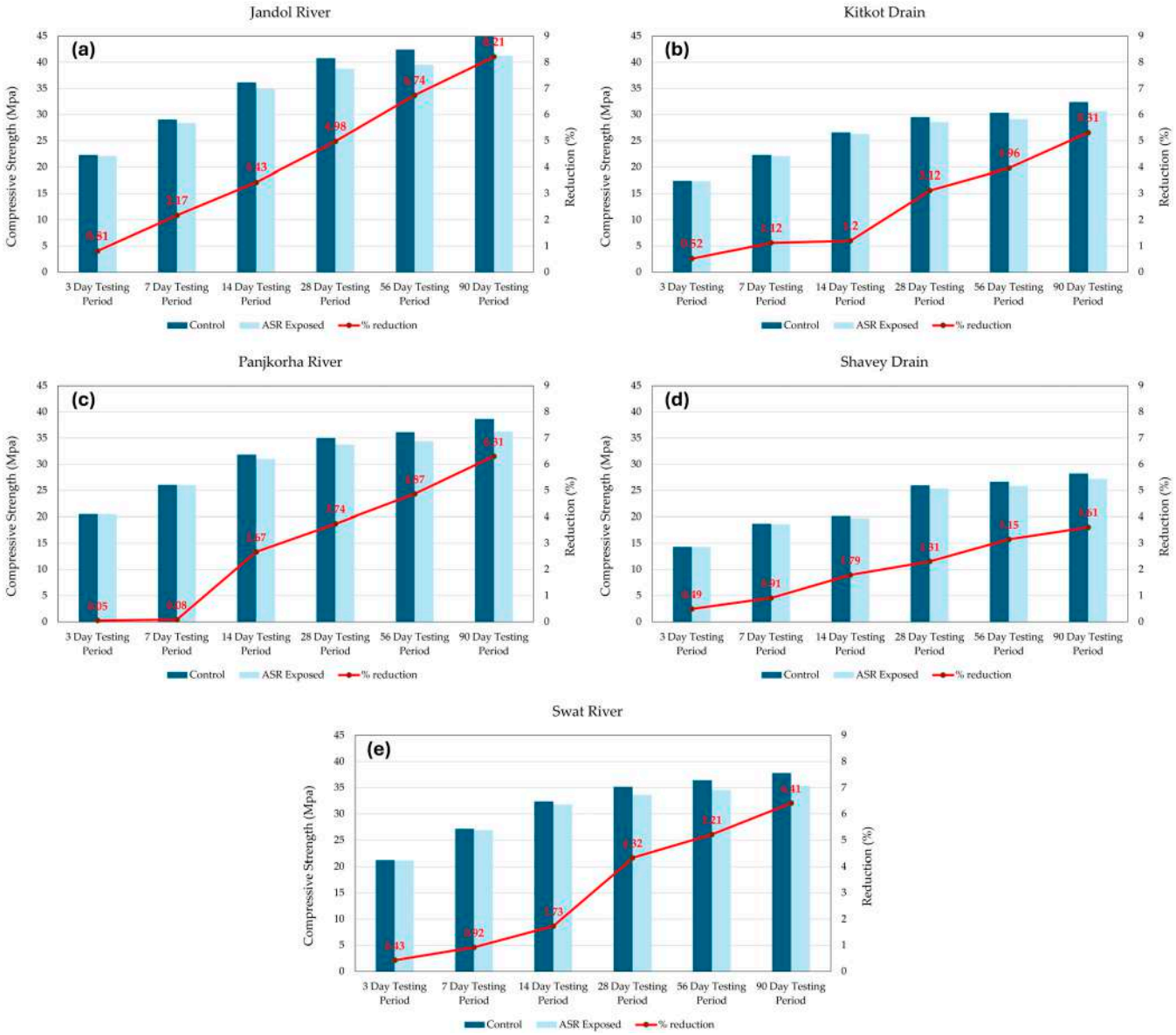

Figure 14. Compressive strength comparison between control and ASR exposed samples: (**a**) Jandol river aggregates; (**b**) Kitkot drain aggregates; (**c**) Panjkorha river aggregates; (**d**) Shavey drain aggregates; (**e**) Swat river aggregates.

3.5. ASR Effect on Modulus of Rupture

Figure 15 illustrates the discrepancy in flexural strength between the control specimens and those subjected to ASR circumstances. The reported flexural strength data give a coefficient of variation (COV) of less than 2.08%, demonstrating the reliability of the results. As the curing time increased resulting from the ongoing hydration process, an expected increase in flexural strength was observed. However, the test results reveal a decrease in flexural strength for prism specimens under ASR conditions in contrast with water cured specimens. For example, Jandol specimens exhibited flexural strengths of 6.03 MPa and 5.75 MPa after 14 days, for the control and ASR affected samples, respectively. In a similar way, the flexural strength of Swat source specimens declined by 1.9% after 14 days. This decrease in flexural strength increased with time. As an example, Kitkot source samples exhibited a 3.84% decline in flexural strength over 28 days and a 6.80% decrease at 90 days in reference to identical samples undergoing water curing. According to Figure 14, the Shavey drain source had the lowest flexural strength at about 5.39 MPa, and the Panjkorha river source had the highest at approximately 8.43 MPa for the samples cured under water.

Notably, Jandol aggregates exhibited a significant decrease of 9.2% and showed a flexural strength of 7.63 MPa under ASR conditions at 90 days, whereas Shavey samples showed the least decrease of 5.6% at the same time interval and showed a flexural strength of 5.09 MPa. Therefore, Shavey drain sources showed less strength loss when tested under ASTM C1260 conditions. Similarly, other aggregate sources tested, namely Swat River, Panjkorha River, and Kitkot drain, also experienced a decline in flexural strength (5.7%, 6.49%, and 6.8% at 14, 28, and 90 days, respectively) when ASR-affected. Earlier investigations have also documented reductions in flexural strength caused by ASR exposure. For instance, Munir et al. [37] experienced a comprehensive loss in flexural strength ranging from 22% to 34% for samples tested under ASR exposure, while Marzouk et al. [39] described a loss of up to 24% linked to moderately reactive aggregates. This study reaffirms that ASR lowers the modulus of rupture, with the degree of reduction correlating with the reactivity of the aggregate source.

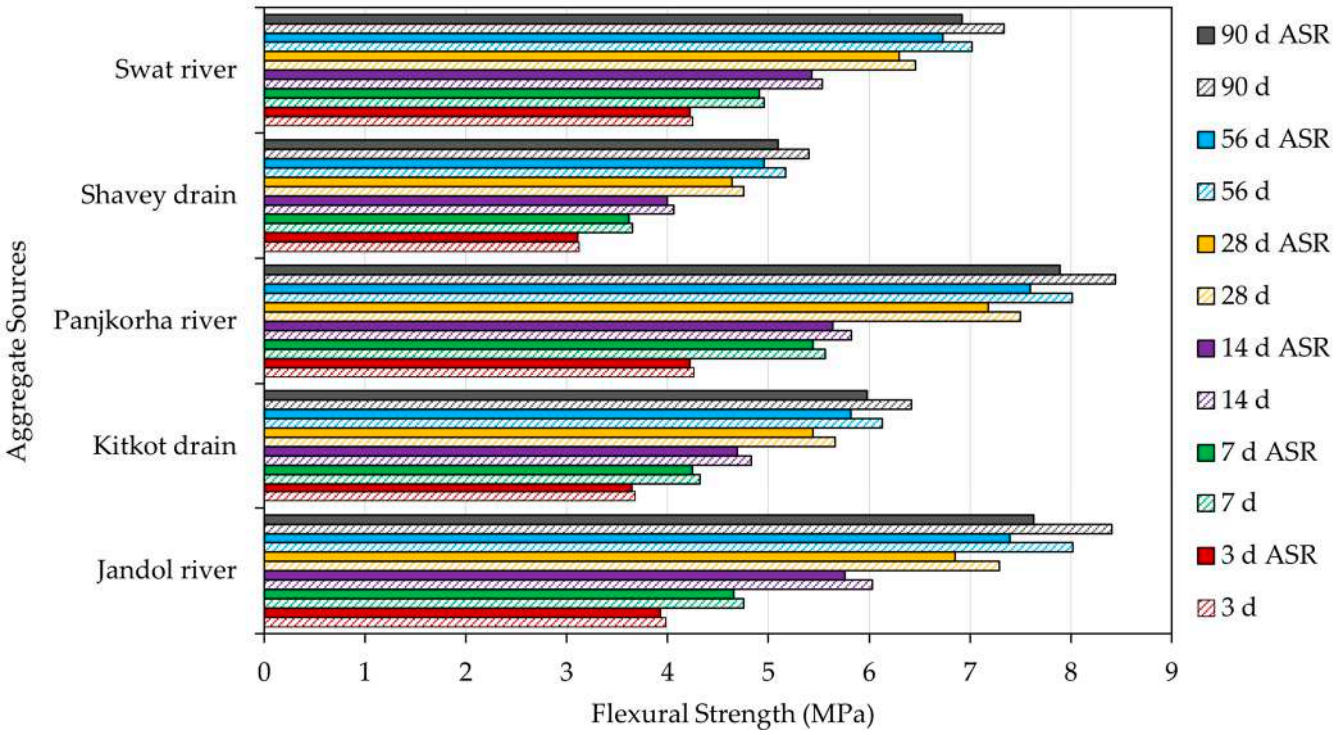

Figure 15. Comparison of flexural strength variation between control samples and ASR affected samples.

Considering the results obtained through this study, the local aggregates sourced from the Jandol River were more susceptible to ASR than aggregates from other sources. This is the point where the ASR mitigation strategies would play their part as discussed earlier. It is not advantageous, rather disastrous, to use these aggregates with Ordinary Portland Cement (OPC). One of the most desirable ASR mitigation strategies recommends using cement containing a lower concentration of alkalis, as the concentration of alkalis and reactive silica directly influences the ASR development in the concrete. Incorporating Supplementary Cementitious Materials (SCMs) such as fly ash, slag cement, silica fume, and natural Pozzolans can also help mitigate the potential of ASR in concrete. Both silica fume and natural pozzolans, such as volcanic ashes, react with alkalis existing in the cement to produce a gel that expands less and thereby resists the development of ASR in concrete. Fly ash also reacts with the alkali to produce a steady gel to mitigate ASR. Other means of manipulating ASR development in concrete are to lower the water-to-cement ratio and apply waterproofing agents to prevent the water from accelerating the conditions that

influence its development; however, detailed evaluation of the concrete mix design and related parameters should not be disregarded.

As discussed above, the availability of water is essential for the ASR process to take place, as it acts as the triggering agent for the alkalis to react with reactive silica. Therefore, the influence of environmental conditions cannot be neglected when discussing ASR mitigation strategies. Areas prone to high humidity pose a greater risk for the ASR development in concrete because it renders the availability of moisture that triggers the degradation process. Usually, in areas that experience heavy rainfall or where there is high humidity, the concrete structures become vulnerable to ASR damage considering the presence of other circumstances that fuel the process. Similar is the effect of temperature that acts as a catalyst to ASR-induced expansion at higher magnitudes since ASR also depends on temperature for its propagation [79]. This is the reason that the structures exposed to direct sunlight in warmer regions experience more ASR-induced damage.

4. Conclusions

In this contribution, the ASR potential of previously unstudied aggregates from a variety of geological sources, including the Panjkorha River, Swat River, Jandol River, Shavey Drain, and Kitkot Drain, was investigated according to ASTM C1260, on which limited literature is available. It was an approach towards sustainable development because ASR is a cancer of concrete that reduces its life span and poses a threat to its duration in time and general existence. Having knowledge of ASR before construction would minimize the resource consumption in the future that would likely occur due to ASR-induced damages. Various investigation techniques, including petrographic analysis, determination of chemical and physical properties, and influence of Alkali–Silica reaction (ASR) on mortar bar expansion and its effects on compressive and flexure strength of cubes and prisms, respectively, were carried out using locally sourced aggregates. It was intended to assist those involved in the construction industry before implementing them into large-scale construction methods.

4.1. Main Outcomes of the Study

The performed analysis yielded the following results:

- Chemical Analysis. The chemical analysis of the cement yielded results that fell within the prescribed limits of ASTM C114. Specifically, the assessment revealed that the cement contained 1.2% free lime, which is well within the standard's limit of no more than 2% for free lime content in cement. The chemical analysis of the aggregates complied with both ASTM and European standards. In particular, the Jandol River and Swat River aggregates had the highest silica content among all the sources, with values of approximately 94.70% and 92.50%, respectively. In addition, the Loss of Ignition values were elevated in all aggregates.
- Physical Analysis. The cement physical characteristics of the conformed to both ASTM and European (EN) standards. Specifically, the fineness and surface area of the cement exceeded ASTM specifications at over 90% and 2250 cm^3/gm, respectively. In addition, the autoclave expansion of the cement, as per ASTM C151 [80], remained well below 0.8%, demonstrating its compliance with established standards. In accordance with ASTM standards, the physical characteristics of all aggregate sources fell within the specified parameters. In particular, Jandool River aggregates exhibited superior resistance to impact, crushing, and abrasion, indicating their robust nature. Conversely, Kitkot Drain aggregates had the lowest impact and crushing values among the tested sources, indicating a lower level of durability. Shavey Drain aggregates, conversely, showed only moderate abrasion resistance.

- Petrographic Analysis. Petrographic examination of the aggregates reveals the presence of reactive minerals, notably peaking at 77% in the Jandool River aggregates, in contrast to minerals from alternative sources that remain within the conventional range. As indicated by ASTM C1260, the Jandool River sample exhibited reactivity, with an expansion of more than 0.2%, while counterparts from other sources exhibited expansions below this threshold after 28 days.
- Compression Test and Flexure Test. The decrease in compressive strength due to ASR exposure varied among samples: Swat River, Panjkorha River, Jandol River, Kitkot Drain, and Shavey Drain, with decreases of 6.40%, 6.32%, 8.22%, 5.31%, and 3.61%, respectively, at the 90-day mark. The reduction in flexural strength under ASR exposure varied among different sources: Swat River, Panjkorha River, Jandool River, Kitkot Drain, and Shavey Drain, exhibiting decreases of 5.7%, 6.49%, 9.2%, 6.8%, and 5.6%, respectively, over the 90-day period.

Based on the above summarized obtained results, aggregates from Kitkot Drain, Shavey Drain, Panjkorha River and Swat River can be considered less susceptible to ASR under accelerated circumstances than aggregates from the Jandol River. Therefore, for aggregates such those sourced from the Jandol River, ASR mitigation strategies like the use of low-alkali-containing cement and the use of SCMs (including fly ash, slag cement, silica fume, and volcanic ashes) are to be contemplated.

4.2. Final Observations and Future Developments

One of the key aspects to consider in this kind of scenario is economic feasibility (along with environmental considerations), which primarily depends on the material and carriage cost, the behavior of the material in the long run, and its reaction to the environmental constraints prevailing in the expected zone of their application. It is suggested to evaluate the aforementioned economic factors along with the chemical and mechanical properties of the possible alternative materials before being considered for large-scale application in a practical field.

From a local viewpoint, this research documentation will help construction companies identify optimal aggregates for concrete construction in the Malakand Division, particularly in hydraulic structures. It will also aid in decision-making regarding preventive measures against ASR issues. The study aims to expand regional aggregate sources without mechanical degradation and minimal environmental impact, addressing energy, environmental, and economic aspects to develop durable materials for sustainable construction. On the other hand, considering a wider perspective, this study represents the initial step of a methodological framework in the context of sustainable development in the construction sector and the promotion of circular economy. Specifically, it involves a preliminary assessment aimed at determining whether locally available materials are structurally suitable for the intended applications, considering both the functional requirements of the structures and the climatic conditions. If the outcome of this initial step is positive (as in the presented study), subsequent phases will include comprehensive environmental and economic analyses, also involving comparisons with conventional alternative materials. The environmental assessments will focus on identifying potential benefits in terms of life cycle analysis, given that local materials generally entail lower environmental impacts during the early stages of sourcing and transportation across production, use, and disposal phases. Additional evaluations will address carbon footprint and pollutant emissions. Economic analyses, on the other hand, will assess the scalability of production, considering both the initial availability of raw materials and the potential for their reuse after the end of the first life cycle, in alignment with circular-economy principles.

Author Contributions: Conceptualization, M.Y., M.S.Z. and M.U. (Muhammad Usman); methodology, M.Y. and M.U. (Muhammad Usman); M.U. (Muhammad Usama) and M.S.Z.; formal analysis, M.U.Y. and M.U. (Muhammad Usama); investigation, M.S.Z.; validation, M.Y., M.U. (Muhammad Usman), M.S.Z., M.U.Y., M.U. (Muhammad Usman), M.S.Z. and M.V.; resources, M.Y., M.S.Z., G.S., L.C. and M.V.; data curation, M.Y., M.S.Z., M.U. (Muhammad Usman), M.U.Y., M.U. (Muhammad Usama), G.S., L.C. and M.V.; writing—original draft preparation, M.Y., M.U. (Muhammad Usman), M.U.Y., M.S.Z., M.U. (Muhammad Usama), L.C. and M.V.; writing—review and editing, M.Y., M.S.Z., M.U. (Muhammad Usman), M.U.Y., M.U. (Muhammad Usama), G.S., L.C. and M.V.; visualization, M.Y., M.S.Z. and M.V.; supervision, M.Y. and M.V. All authors have read and agreed to the published version of the manuscript.

Funding: This research received no external funding.

Institutional Review Board Statement: Not applicable.

Informed Consent Statement: Not applicable.

Data Availability Statement: The data that support the findings of this study are available from the corresponding author upon reasonable request.

Conflicts of Interest: The authors declare no conflicts of interest.

References

1. Triassi, M.; Alfano, R.; Illario, M.; Nardone, A.; Caporale, O.; Montuori, P. Environmental Pollution from Illegal Waste Disposal and Health Effects: A Review on the "Triangle of Death". *Int. J. Environ. Res. Public. Health* **2015**, *12*, 1216–1236. [CrossRef]
2. Cirrincione, L.; La Gennusa, M.; Peri, G.; Rizzo, G.; Scaccianoce, G. The Landfilling of Municipal Solid Waste and the Sustainability of the Related Transportation Activities. *Sustainability* **2022**, *14*, 5272. [CrossRef]
3. Vocciante, M.; Meshalkin, V. An Accurate Inverse Model for the Detection of Leaks in Sealed Landfills. *Sustainability* **2020**, *12*, 5598. [CrossRef]
4. Cachada, A.; Rocha-Santos, T.; Duarte, A.C. Soil and Pollution. In *Soil Pollution*; Elsevier: Amsterdam, The Netherlands, 2018; pp. 1–28.
5. Yang, Y.; Zhou, C.; Peng, J.; Li, H.; Dong, Y.; Cai, C.S. Theory-Informed Deep Neural Network-Based Time-Dependent Flexural Reliability Assessment of Corroded PC Structures. *Eng. Struct.* **2025**, *329*, 119819. [CrossRef]
6. Farhadian, M.; Vachelard, C.; Duchez, D.; Larroche, C. In Situ Bioremediation of Monoaromatic Pollutants in Groundwater: A Review. *Bioresour. Technol.* **2008**, *99*, 5296–5308. [CrossRef]
7. Pietrelli, L.; Ferro, S.; Reverberi, A.P.; Vocciante, M. Removal of Polyethylene Glycols from Wastewater: A Comparison of Different Approaches. *Chemosphere* **2021**, *273*, 129725. [CrossRef] [PubMed]
8. de Folly d'Auris, A.; Rubertelli, F.; Taini, A.; Vocciante, M. A Novel Polyurethane-Based Sorbent Material for Oil Spills Management. *J. Environ. Chem. Eng.* **2023**, *11*, 111386. [CrossRef]
9. Liu, Y.; Fei, Y.; Li, Y.; Bao, X.; Zhang, P. A Review of the Pollution Source Identification Methods and Remediation Technologies of Groundwater. *China Geol.* **2022**, *7*, 125–137. [CrossRef]
10. ZAFAR, M.S.; Gatto, F.; Mancini, G.; Lauciello, S.; Pompa, P.; Athanassiou, A.; Fragouli, D. Biocomposite Cryogels for Photothermal Decontamination of Water. *Langmuir* **2023**, *39*, 7793–7803. [CrossRef]
11. Khan, F.I.; Husain, T.; Hejazi, R. An Overview and Analysis of Site Remediation Technologies. *J. Environ. Manag.* **2004**, *71*, 95–122. [CrossRef]
12. Pedron, F.; Grifoni, M.; Barbafieri, M.; Petruzzelli, G.; Franchi, E.; Samà, C.; Gila, L.; Zanardi, S.; Palmery, S.; Proto, A.; et al. New Light on Phytoremediation: The Use of Luminescent Solar Concentrators. *Appl. Sci.* **2021**, *11*, 1923. [CrossRef]
13. Conte, A.; Chiaberge, S.; Pedron, F.; Barbafieri, M.; Petruzzelli, G.; Vocciante, M.; Franchi, E.; Pietrini, I. Dealing with Complex Contamination: A Novel Approach with a Combined Bio-Phytoremediation Strategy and Effective Analytical Techniques. *J. Environ. Manag.* **2021**, *288*, 112381. [CrossRef] [PubMed]
14. Song, P.; Xu, D.; Yue, J.; Ma, Y.; Dong, S.; Feng, J. Recent Advances in Soil Remediation Technology for Heavy Metal Contaminated Sites: A Critical Review. *Sci. Total Environ.* **2022**, *838*, 156417. [CrossRef]
15. Zafar, M.S.; Zahid, M.; Athanassiou, A.; Fragouli, D. Biowaste-Derived Carbonized Bone for Solar Steam Generation and Seawater Desalination. *Adv. Sustain. Syst.* **2021**, *5*, 2100031. [CrossRef]
16. Voit, K.; Zeman, O.; Janotka, I.; Adamcova, R.; Bergmeister, K. High-Durability Concrete Using Eco-Friendly Slag-Pozzolanic Cements and Recycled Aggregate. *Appl. Sci.* **2020**, *10*, 8307. [CrossRef]

17. Yagüe, S.; Rosales-Prieto, V.; Sánchez-Lite, A.; González-Gaya, C. Properties of Green Mortar Containing Granite Sawmill. *Appl. Sci.* **2021**, *11*, 2136. [CrossRef]
18. Hatami Shirkouh, A.; Meftahi, F.; Soliman, A.; Godbout, S.; Palacios, J. Performance of Eco-Friendly Zero-Cement Particle Board under Harsh Environment. *Appl. Sci.* **2024**, *14*, 3118. [CrossRef]
19. Cirrincione, L.; Gennusa, M.L.; Peri, G.; Rizzo, G.; Scaccianoce, G. Foster Carbon-Neutrality in the Built Environment: A Blockchain-Based Approach for the Energy Interaction Among Buildings. In Proceedings of the 2022 Workshop on Blockchain for Renewables Integration (BLORIN), Palermo, Italy, 2–3 September 2022; pp. 167–171.
20. Llorach-Massana, P.; Cirrincione, L.; Sierra-Perez, J.; Scaccianoce, G.; Gennusa, M.L.; Peña, J.; Rieradevall, J. Environmental Assessment of a New Building Envelope Material Derived from Urban Agriculture Wastes: The Case of the Tomato Plants Stems. *Int. J. Life Cycle Assess.* **2023**, *28*, 813–827. [CrossRef]
21. Yang, Y.; Chen, H.; Peng, J.; Dong, Y. Machine Learning-Based Probabilistic Prediction Model for Chloride Concentration in the Interfacial Zone of Precast and Cast-in-Place Concrete Structures. *Structures* **2025**, *72*, 108224. [CrossRef]
22. Capitano, C.; Cirrincione, L.; Peri, G.; Rizzo, G.; Scaccianoce, G. A Simplified Method for the Indirect Evaluation of the "Embodied Pollution" of Natural Stones (Marble) Working Chain to Be Applied for Achieving the Ecolabel Brand of the Product. *J. Clean. Prod.* **2022**, *362*, 132576. [CrossRef]
23. Fanijo, E.O.; Kolawole, J.T.; Almakrab, A. Alkali-Silica Reaction (ASR) in Concrete Structures: Mechanisms, Effects and Evaluation Test Methods Adopted in the United States. *Case Stud. Constr. Mater.* **2021**, *15*, 563. [CrossRef]
24. Tosun, K.; Felekoğlu, B.; Baradan, B. The Effect of Cement Alkali Content on ASR Susceptibility of Mortars Incorporating Admixtures. *Build. Environ.* **2007**, *42*, 3444–3453. [CrossRef]
25. Mo, K.H.; Ling, T.-C.; Tan, T.H.; Leong, G.W.; Yuen, C.W.; Shah, S.N. Alkali-Silica Reactivity of Lightweight Aggregate: A Brief Overview. *Constr. Build. Mater.* **2021**, *270*, 121444. [CrossRef]
26. Ichikawa, T.; Miura, M. Modified Model of Alkali-Silica Reaction. *Cem. Concr. Res.* **2007**, *37*, 1291–1297. [CrossRef]
27. Stanton, T.E. Expansion of Concrete through Reaction between Cement and Aggregate. *Trans. Am. Soc. Civil. Eng.* **1942**, *107*, 54–84. [CrossRef]
28. Chrisp, T.M.; Waldron, P.; Wood, J.G.M. Development of a Non-Destructive Test to Quantify Damage in Deteriorated Concrete. *Mag. Concr. Res.* **1993**, *45*, 247–256. [CrossRef]
29. Peri, G.; Cirrincione, L.; Mazzeo, D.; Matera, N.; Scaccianoce, G. Building Resilience to a Warming World: A Contribution toward a Definition of "Integrated Climate Resilience" Specific for Buildings—Literature Review and Proposals. *Energy Build.* **2024**, *315*, 114319. [CrossRef]
30. Peri, G.; Licciardi, G.R.; Matera, N.; Mazzeo, D.; Cirrincione, L.; Scaccianoce, G. Disposal of Green Roofs: A Contribution to Identifying an "Allowed by Legislation" End–of–Life Scenario and Facilitating Their Environmental Analysis. *Build. Environ.* **2022**, *226*, 109739. [CrossRef]
31. Thomas, M.D.A.; Innis, F.A. Effect of Slag on Expansion Due to Alkali Aggregate Reaction in Concrete. *ACI Mater J.* **1998**, *95*, 716–724. [CrossRef]
32. Shafaatian, S.M.H.; Akhavan, A.; Maraghechi, H.; Rajabipour, F. How Does Fly Ash Mitigate Alkali–Silica Reaction (ASR) in Accelerated Mortar Bar Test (ASTM C1567)? *Cem. Concr. Compos.* **2013**, *37*, 143–153. [CrossRef]
33. Shehata, M.H.; Thomas, M.D.A. Use of Ternary Blends Containing Silica Fume and Fly Ash to Suppress Expansion Due to Alkali–Silica Reaction in Concrete. *Cem. Concr. Res.* **2002**, *32*, 341–349. [CrossRef]
34. Lumley, J.S. ASR Suppression by Lithium Compounds. *Cem. Concr. Res.* **1997**, *27*, 235–244. [CrossRef]
35. Luo, D.; Sinha, A.; Adhikari, M.; Wei, J. Mitigating Alkali-Silica Reaction through Metakaolin-Based Internal Conditioning: New Insights into Property Evolution and Mitigation Mechanism. *Cem. Concr. Res.* **2022**, *159*, 106888. [CrossRef]
36. Godart, B.; de Rooij, M.R.; Wood, J.G. *Guide to Diagnosis and Appraisal of AAR Damage to Concrete in Structures*; Springer: Dordrecht, The Netherlands, 2013.
37. Munir, M.J.; Abbas, S.; Qazi, A.U.; Nehdi, M.L.; Kazmi, S.M.S. Role of Test Method in Detection of Alkali–Silica Reactivity of Concrete Aggregates. *Proc. Inst. Civil. Eng. Constr. Mater.* **2018**, *171*, 203–221. [CrossRef]
38. *C1260-23*; Standard Test Method for Potential Alkali Reactivity of Aggregates (Mortar-Bar Method). ASTM: West Conshohocken, PA, USA, 2007.
39. Marzouk, H.; Langdon, S. The Effect of Alkali-Aggregate Reactivity on the Mechanical Properties of High and Normal Strength Concrete. *Cem. Concr. Compos.* **2003**, *25*, 549–556. [CrossRef]
40. Islam, M.S.; Ghafoori, N. Relation of ASR-Induced Expansion and Compressive Strength of Concrete. *Mater. Struct.* **2015**, *48*, 4055–4066. [CrossRef]
41. Na, O.; Xi, Y.; Ou, E.; Saouma, V.E. The Effects of Alkali-Silica Reaction on the Mechanical Properties of Concretes with Three Different Types of Reactive Aggregate. *Struct. Concr.* **2016**, *17*, 74–83. [CrossRef]
42. Oberholster, R.E.; Davies, G. An Accelerated Method for Testing the Potential Alkali Reactivity of Siliceous Aggregates. *Cem. Concr. Res.* **1986**, *16*, 181–189. [CrossRef]

43. *C227*; Standard Test Method for Potential Alkali Reactivity of Cement-Aggregate Combinations (Mortar-Bar Method). ASTM: West Conshohocken, PA, USA, 2018.
44. Abbas, S.; Hussain, I.; Aslam, F.; Ahmed, A.; Gillani, S.A.A.; Shabbir, A.; Deifalla, A.F. Potential of Alkali–Silica Reactivity of Unexplored Local Aggregates as per ASTM C1260. *Materials* **2022**, *15*, 6627. [CrossRef]
45. Hassan, E.U.L.; Hannan, A.; Rashid, M.U.R.; Ahmed, W.; Zeb, M.J.; Khan, S.; Abbas, S.A.; Ahmad, A. Resource Assessment of Sakesar Limestone as Aggregate from Salt Range Pakistan Based on Geotechnical Properties. *Int. J. Hydrol.* **2020**, *4*, 24–29. [CrossRef]
46. Hakim, R.; Mehmood, K.; Ahad, M.Z.; Hakim, I. Engineering Characterization of Course Aggregate Used in Cement Concrete from Local Quarries in Dir (Lower), KP, Pakistan. *Int. J. Sci. Eng. Res.* **2018**, *9*, 1–6.
47. Pathan, M.A.; Lashae-Ri, R.A.; Maira, M.; Professor, A.; Professor, A. A Study on Types and Quality of Aggregates Produced in LONI KOT Karachi-Hyderabad Motorway Used in Building Construction. *Int. J. Eng. Sci. Comput.* **2018**, *8*, 17870.
48. Munir, M.J.; Kazmi, S.M.S.; Wu, Y.-F. Efficiency of Waste Marble Powder in Controlling Alkali–Silica Reaction of Concrete: A Sustainable Approach. *Constr. Build. Mater.* **2017**, *154*, 590–599. [CrossRef]
49. Munir, M.J.; Abbas, S.; Minhaj, S.; Kazmi, S.; Khitab, A.; Ashiq, S.Z.; Arshad, M.T. Engineering Characteristics of Widely Used Coarse Aggregates in Pakistan: A Comparative Study. *Pak. J. Engg. Appl. Sci.* **2017**, *20*, 85–93.
50. Naseem, S.; Hussain, K.; Shahab, B.; Bashir, E.; Bilal, M.; Hamza, S. Investigation of Carbonate Rocks of Malikhore Formation as Coarse Aggregate and Dimension Stone, SE Balochistan, Pakistan. *Br. J. Appl. Sci. Technol.* **2016**, *12*, 1–11. [CrossRef]
51. Qureshi, M.A.; Aslam, M.; Shah, A.N.R.; Otho, S.H. Influence of Aggregate Characteristics on the Compressive Strength. *Tech. J. Univ. Eng. Technol. Taxila* **2015**, *20*, 1–10.
52. Naeem, M.; Khalid, P.; Sanaullah, M.; ud Din, Z. Physio-Mechanical and Aggregate Properties of Limestones from Pakistan. *Acta Geod. Geophys.* **2014**, *49*, 369–380. [CrossRef]
53. Siddiqi, Z.A.; Hameed, R.; Saleem, M.; Khan, Q.S.; Ishaq, I. Performance Study of Locally Available Coarse Aggregates of Azad Kashmir. *Pak. J. Sci.* **2013**, *65*, 90–94.
54. Ayub, M.; Shahzada, K.; Profile, S.; Naseer, A.; Shoaib, M. Engineering Assessment of Coarse Aggregates Used in Peshawar. *Int. J. Adv. Struct. Geotech. Eng.* **2012**, *1*, 61–64.
55. Gondal, M.M.I.; Ahsan, N.; Javid, A.Z. Engineering Properties of Potential Aggregate Resources from Eastern and Central Salt Range, Pakistan. *Geol. Bull. Punjab Univ.* **2009**, *44*, 97–103.
56. Ahsan, N.; Chaudhry, M.N.; Gondal, M.M.I.; Khan, Z.K. Allai Aggregate for Rehabilitation and Reconstruction of October 8, 2005 Earthquake Affected Allai-Banan Area, NWFP, Pakistan. *Geol. Bull. Punjab Univ.* **2009**, *44*, 1–12.
57. Gondal, M.M.I.; Ahsan, N.; Javid, A.Z. Evaluation of Shaki Sarwar and Rajan Pur Aggregates for Construction in Southern Punjab Province, Pakistan. *Geol. Bull. Punjab Univ.* **2008**, *43*, 101–107.
58. Kamal, M.A.; Sulehri, M.A.; Hughes, D.A.B. Engineering Characteristics of Road Aggregates from Northern Pakistan and the Development of a Toughness Index. *Geotech. Geol. Eng.* **2006**, *24*, 819–831. [CrossRef]
59. *Cement–Part 1, Composition, Specifications and Conformity Criteria for Common Cements*; BSI: Herndon, VA, USA, 2000; ISBN 0580364569.
60. *ASTM C204*; Standard Test Methods for Fineness of Hydraulic Cement by Air-Permeability Apparatus. ASTM: West Conshohocken, PA, USA, 2023.
61. *ASTM C184-94e1*; Standard Test Method for Fineness of Hydraulic Cement by the 150-µm (No. 100) and 75-µm (No. 200) Sieves (Withdrawn 2002). ASTM: West Conshohocken, PA, USA, 2002.
62. *ASTM C191-21*; Standard Test Methods for Time of Setting of Hydraulic Cement by Vicat Needle. ASTM: West Conshohocken, PA, USA, 2021.
63. *ASTM C187-16*; Standard Test Method for Amount of Water Required for Normal Consistency of Hydraulic Cement Paste. ASTM: West Conshohocken, PA, USA, 2023.
64. Kamani, M.; Ajalloeian, R. Evaluation of the Mechanical Degradation of Carbonate Aggregate by Rock Strength Tests. *J. Rock. Mech. Geotech. Eng.* **2019**, *11*, 121–134. [CrossRef]
65. Mohajerani, A.; Nguyen, B.T.; Tanriverdi, Y.; Chandrawanka, K. A New Practical Method for Determining the LA Abrasion Value for Aggregates. *Soils Found.* **2017**, *57*, 840–848. [CrossRef]
66. *ASTM C535-16*; Standard Test Method for Resistance to Degradation of Large-Size Coarse Aggregate by Abrasion and Impact in the Los Angeles Machine. ASTM: West Conshohocken, PA, USA, 2024.
67. *ASTM C29/C29M-97*; Standard Test Method for Bulk Density ("Unit Weight") and Voids in Aggregate. ASTM: West Conshohocken, PA, USA, 2023.
68. *ASTM C127-15*; Standard Test Method for Relative Density (Specific Gravity) and Absorption of Coarse Aggregate (Withdrawn 2024). ASTM: West Conshohocken, PA, USA, 2024.
69. *ASTM C114-18*; Standard Test Methods for Chemical Analysis of Hydraulic Cement. ASTM: West Conshohocken, PA, USA, 2022.

70. *ASTM C295-08*; Standard Guide for Petrographic Examination of Aggregates for Concrete. ASTM: West Conshohocken, PA, USA, 2011.
71. *ASTM C109/C109M-20*; Standard Test Method for Compressive Strength of Hydraulic Cement Mortars (Using 2-in. or [50-Mm] Cube Specimens). ASTM: West Conshohocken, PA, USA, 2020.
72. *ASTM C348-21*; Standard Test Method for Flexural Strength of Hydraulic-Cement Mortars. ASTM: West Conshohocken, PA, USA, 2021.
73. *ASTM C490/C490M-21*; Standard Practice for Use of Apparatus for the Determination of Length Change of Hardened Cement Paste, Mortar, and Concrete. ASTM: West Conshohocken, PA, USA, 2021.
74. Leemann, A.; Le Saout, G.; Winnefeld, F.; Rentsch, D.; Lothenbach, B. Alkali–Silica Reaction: The Influence of Calcium on Silica Dissolution and the Formation of Reaction Products. *J. Am. Ceram. Soc.* **2011**, *94*, 1243–1249. [CrossRef]
75. Teo, B.K.; Sun, X.H. Silicon-Based Low-Dimensional Nanomaterials and Nanodevices. *Chem. Rev.* **2007**, *107*, 1454–1532. [CrossRef]
76. Polyakova, I.G. 4. The Main Silica Phases and Some of Their Properties. In *Selected Properties and Crystallization*; Schmelzer, J.W.P., Ed.; De Gruyter: Berlin, Germany; Boston, MA, USA, 2014; pp. 197–268. ISBN 9783110298581.
77. Robert, J. Dunham Classification of Carbonate Rocks According to Depositional Textures. In *The AAPG/Datapages Combined Publications Database*; American Association of Petroleum Geologists: Washington, WA, USA, 1962.
78. Forster, S.W.; Akers, D.J.; Lee, M.K.; Pergalsky, A.; Arrand, C.D.; Lewis, D.W.; Pierce, J.S.; Barger, G.S.; Macdonald, D.R.; Pisaneschi, R.R.; et al. *State-of-the-Art Report on Alkali-Aggregate Reactivity*; American Concrete Institute: Farmington Hills, MI, USA, 1998.
79. Stark, D. *Eliminating or Minimizing Alkali-Silica Reactivity*; Strategic Highway Research Program, National Research Council: Washington, DC, USA, 1993; ISBN 0309056039.
80. *ASTM C151*; Standard Test Method for Autoclave Expansion of Hydraulic Cement. ASTM International: West Conshohocken, PA, USA, 2015.